ASSESSING THE EFFECT OF TEMPERATURE ON *STREPTOMYCES GRISEU*S GROWTH AND METABOLISM

by

Tyler Rodshagen

A Thesis Submitted to the Faculty of the

DEPARTMENT OF ENVIRONMENTAL SCIENCE

In Partial Fulfillment of the Requirements

For the Degree of

MASTER OF SCIENCE

WITH A MAJOR IN ENVIRONMENTAL SCIENCE

In the Graduate College

THE UNIVERSITY OF ARIZONA

2022

THE UNIVERSITY OF ARIZONA
GRADUATE COLLEGE

As members of the Master's Committee, we certify that we have read the thesis prepared by Tyler Rodshagen, titled Assessing the Effect of Temperature on *Streptomyces griseus* Growth and Metabolite Production and recommend that it be accepted as fulfilling the dissertation requirement for the Master's Degree.

Malak Tfaily Date: 5.12.22

Jean McLain Date: 5.11.22

Luisa Ikner Date: 5.11.22

Final approval and acceptance of this thesis is contingent upon the candidate's submission of the final copies of the thesis to the Graduate College.

I hereby certify that I have read this thesis prepared under my direction and recommend that it be accepted as fulfilling the Master's requirement.

Malak Tfaily Date: 5.12.22
Master's Thesis Committee Chair
Department of Environmental Science

Table of Contents

List of Figures

List of Tables

Abstract

With the current rate of population growth, it is estimated that global food production will need to double over the course of the next century to sustain healthy diets on the global scale. Given the limited amount of arable land that could be used for agriculture, gains in crop production will need to come from improving current practices rather than from expanding farmlands. The Food and Agriculture Organization (FAO) estimates that 20-40% of yearly crop losses can be attributed to pests, with the majority of damages coming from pathogens. Rhizobacteria like *Streptomyces griseus* can defend plants from pathogens and even promote plant growth, but it is unknown how this bacterium's growth and metabolism will respond to rising global temperatures. We used a combination of high resolution FTICR-MS and LC-MS/MS to assess changes in bacterial metabolism (including primary and secondary metabolites) as a function of increasing temperature. Analysis of microbial growth curves and metabolomics data revealed that microbial activity, metabolite abundance/diversity, and the production of compounds beneficial to plants were greatest at 22 ˚C, intermediate at 35 ˚C, with practically no activity at 4 ℃. These results suggest that as global temperatures rise, *S. griseus* may confer fewer benefits to plants. If other rhizobacteria respond in similar ways, current methods of pest and pathogen control must be improved, or new methods must be developed, to reduce crop losses to pathogens. Reducing crop losses to pathogens will be paramount to ensure that global food security is achieved by the end of the century and beyond.

Chapter 1: Background Information

1.1 Current State of Agriculture and Global Food Security

With the global population expected to increase by two billion people over the next 30 years, producing enough food to ensure global food security is a challenge that humanity will have to learn to overcome in the near future (UN, 2019). Food security is defined as the "situation when there is sufficient food to meet dietary needs for an active, healthy life, and may be considered on the global, national, community, or household level". There are many areas in the world where this is already a problem (Mahmuti et al., 2009). According to the United Nations, one in three people did not have sufficient access to food in 2020 (Figure 1) (UN, 2021). While these numbers may be in part fueled by the coronavirus disease 2019 pandemic (COVID-19), it is likely that the proportion of hunger will increase as time progresses because the majority of the projected population growth will come from developing countries that are home to many subsistence farmers who may already struggle with household food security (Mahmuti et al., 2009; UN, 2019).

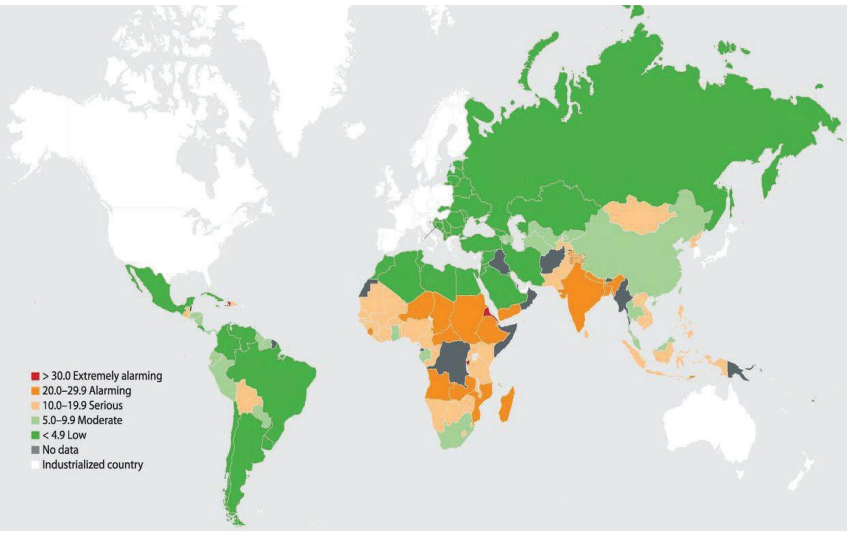

Figure 1. Global distribution of hunger in 2012. Degree of hunger by country was calculated using the equally weighted proportions of people who are undernourished, the proportion of children under 5 who are underweight, and the mortality rate of children younger than age 5 (Wheeler & Braun, 2013).

In order to meet the nutritional demands of an ever-increasing human population, some studies project that food production will soon need to double (Lomba et al., 2019). Although there is some time to scale up farming practices, doubling agricultural production is not a simple task. One of the main issues with increasing food production under current practices is that almost 40% of Earth's terrestrial surface is already devoted to agriculture (Lomba et al., 2019). Given that less than 100% of Earth's terrestrial surface is viable for crop production and the rising population increases the demand for other land uses like housing, there is limited room to expand farmland under current practices (FAO, 2003). In 2015, Food and Agriculture Organization published a "road map" that outlines various challenges in the context of global food security (Figure 2). In addition to the challenges outlined in Figure 2, the FAO describes other issues such as agriculture derived greenhouse gas emissions exacerbating climate change, climate change jeopardizing crop production, and observed increases in transboundary disease and pest outbreaks (FAO, 2019). All of these issues, and more, will need to be addressed to achieve food security on a global scale.

Pests such as insects and pathogens are responsible for 20-40% of all crop losses, amounting to roughly $300 billion lost worldwide each year (FAO, 2019). Of this percentage, over 70% of the losses are directly caused by pathogens (FAO, 2019). There are multiple approaches to reduce crop losses to pests, but most of these approaches have disadvantages. One approach is to use pesticides and other agrochemicals to kill pests before they have an opportunity to cause damage (Lugtenberg & Kamilova, 2009). While these chemicals are effective for killing insects and pathogens, many of these compounds have side effects that are potentially harmful to the environment, making them unpopular with consumers and governments (Lugtenberg & Kamilova, 2009). Another approach is to genetically modify plants for resistance to specific

diseases, but similar to the use of agrochemicals, this method is unpopular with many consumers and governments (Lugtenberg & Kamilova, 2009). Another downside to crops that are engineered for pathogen resistance is that they require an extended period to cultivate and may not retain their resistance for a valuable length of time (Mahmuti et al., 2009). An example of this is the cultivation of a commercial rapeseed cultivar that was resistant to the fungal pathogen *Leptosphaeria maculans*. The cultivar took ten years to develop but only two years to become ineffective (Mahmuti et al., 2009). A similar approach to genetically modifying crops is selectively breeding for plants that have acquired immunity to one or more diseases (Lugtenberg & Kamilova, 2009). Because there is no human mediated genetic modification involved, this method is more accepted among consumers and governments, but similar to genetic engineering it takes a long time to cultivate and scale (Lugtenberg & Kamilova, 2009). First a crop must express resistance to a pathogen and then it has to be produced in mass through a series of cross breeding, both of which are time-consuming processes (Poland & Rutkoski, 2016). Given that agricultural production must be scaled up relatively quickly, the time that must be invested in these approaches for them to be effective could prove problematic, at least in the short term.

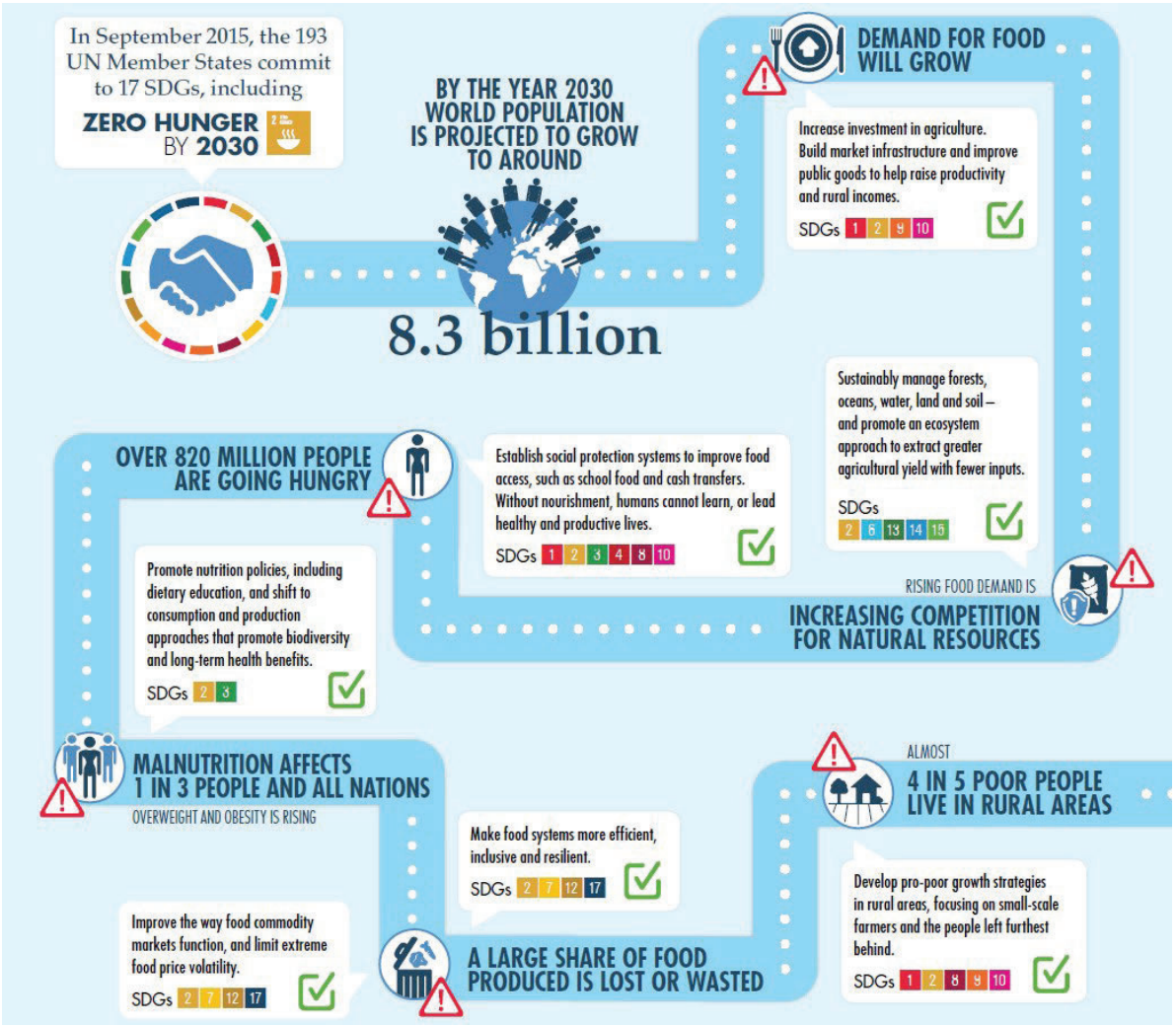

Figure 2. FAO roadmap outlining challenges that contribute to food inequality and issues that must be addressed to end global hunger by 2030 (SDG = sustainable development goal) (FAO, 2019).

1.2 Introduction to *Streptomyces griseus*

In contrast to the approaches discussed above, the rhizosphere microbiome may hold the key to reducing crop losses to pathogens. Over 100 years ago, Lorenz Hiltner defined the rhizosphere as "the soil compartment influenced by plant roots" (Bakker et al., 2013). Since then, research into the rhizosphere microbiome has flourished and it is now known that the concentration of bacteria in the rhizosphere is 10-1000 times greater than in bulk soil because plants exude large amounts of organic carbon (Lugtenberg & Kamilova, 2009; Bakker et al., 20013). There is great diversity among microorganisms in the rhizosphere, with some providing benefits to the plants, some causing disease, and others that are neutral in regard to the plant but pathogenic to humans (Mendes et al., 2013).

Microorganisms in the rhizosphere can benefit plants through physical and chemical mechanisms linked to processes like biofertilization, root growth promotion, response to abiotic stress, and disease control (Mendes et al., 2013). Microorganisms in the rhizosphere can promote root growth and biofertilization by aiding in the acquisition of limiting macro nutrients, acquiring trace elements such as iron through siderophores, and excreting plant growth regulators (auxins) (Mendes et al., 2013). Rhizobacteria use a variety of methods to defend plants against soil pathogens such as antibiosis (e.g. antibiotic production), competing for macro nutrients and trace elements, forming parasitic relationships with pathogens, interfering with virulent quorum sensing, and inducing systemic resistance in the plant (Mendes et al., 2013).

Chemical mechanisms of plant growth promotion and protection are mainly achieved through the production of secondary metabolites such as antibiotics, volatile organic compounds, siderophores, auxins, and enzymes (Mendes et al., 2013). One class of bacteria that are well known for secondary metabolite production are Actinobacteria, from which two-thirds of naturally occurring antibiotics have been isolated (Olanrewaju & Babalola, 2019). Within the class Actinobacteria, the genus *Streptomyces* is responsible for 75% of the isolated antibiotics (Olanrewaju & Babalola, 2019). *Streptomyces* spp. are found in many types of soil from polar territories to deserts to marine sediments (Sottorf et al., 2019). Most species within this genus of rhizobacteria require oxygen to grow, but some are able to grow anaerobically (Olanrewaju & Babalola, 2019).

Volatile organic compounds (VOCs) can be defined as substances with a molecular weight less than 300 Daltons (Da) with low polarity and a high vapor pressure, such as alkanes, ketones, acids, and esters (Danaei et al., 2014). VOCs are adept at preventing the proliferation of fungi because they can prevent mycelium growth and inhibit spore germination, limiting the spread and reproduction of fungi (Danaei et al., 2014). There is also evidence that VOCs can affect plant growth and may be involved in microbe-microbe and microbe-plant interactions (Mendes et al., 2013). This communication is important because these quorum sensing molecules can cause plants to activate genes that are beneficial for defending against pathogens and abiotic stressors (Mendes et al., 2013).

Other secondary metabolites produced by *Streptomyce*s that benefit plants are plant growth regulators and siderophores. An example of a plant growth regulator produced by *Streptomyces* is indole-3-acetic acid, an auxin that promotes plant growth by stimulating cell elongation and division (Vurukonda et al., 2018). Siderophores aid in the transport of iron from soil to plants (BioLibreTexts, 2021). Siderophores are important to plants because despite the naturally high concentration of iron in most soils, the majority of it is present in a low solubility form and is therefore not immediately available to plants (Mendes et al., 2013).

Streptomyces secrete a variety of enzymes that help plants in numerous ways. Chitinase and other lytic enzymes are capable of defending plants against fungal diseases such as *Fusarium oxysporum*, *Fusarium solani*, *Alternaria alternata*, and *Rhizoctonia solani* (Danaei et al., 2014). Other enzymes are able to promote plant growth by breaking down insoluble organic polymers such as chitin and cellulose into simple sugars that plants can take up through ATP-binding cassette (ABC) transporters (Vurukonda et al., 2018).

In addition to producing secondary metabolites, *Streptomyces* have physical means of protecting plants against disease and promoting growth. *Streptomyces* are filamentous bacteria that sporulate and grow

long filaments called hyphae with multiple nuclei that elongate from the center of the colony by apical growth (Olanrewaju & Babalola, 2019). Hyphae can promote plant growth by aiding in nutrient acquisition (Vurukonda et al., 2018). There are multiple mechanisms in which hyphae can prevent pathogens from infecting a plant. Close to the roots, hyphae are wide-spreading and occupy extensive space surrounding plant roots, allowing them to outcompete many other microorganisms (Olanrewaju & Babalola, 2019). The space required by *Streptomyces* hyphae can be sufficient to prevent pathogens from colonizing plant roots and it blocks pathogen access to nutrients secreted by the plant (Olanrewaju & Babalola, 2019). Additionally, hyphae improve nutrient use efficiency by better colonizing nutrient rich substrate, which also helps *Streptomyces* outcompete pathogens (Olanrewaju & Babalola, 2019).

In addition to hyphae, the spores produced by *Streptomyces* play a role in preventing plant diseases and promoting growth. Sporulation causes a bacterial colony to strongly adhere to rhizosphere soil particles, allowing for enhanced microbe-plant interactions (Olanrewaju & Babalola, 2019). This strong bond combined with wide-spreading hyphae means that the bacteria has increased resilience to biotic and abiotic stressors (Olanrewaju & Babalola, 2019). This resilience is important for plants because it means that even in times of stress the bacteria can continue to protect the plant and promote growth. These traits allow *Streptomyces* to outcompete most other microorganisms during times of stress in the soil environment (Olanrewaju & Babalola, 2019). Without these traits, pathogens might outcompete *Streptomyces* in the soil and cause further stress to the plant.

Within the *Streptomyces* genus, one species of particular interest is *Streptomyces griseus*. *S. griseus* is a globally ubiquitous and well-characterized rhizobacterium that is best known for producing the antibiotic streptomycin (Vurukonda et al., 2018). Streptomycin was the first aminoglycoside antibiotic to be discovered and has been used since its discovery to treat bacterial infections in humans (Waters & Tadi, 2021). It has a similar function in plants, preventing diseases such as bacterial rots, cankers, and blight (Vurukonda et al., 2018; Lang et al., 2019). Streptomycin has been shown to prevent these types of infections in pome fruits, stone fruits, citrus fruits, vegetables, potatoes, tobacco, cotton, ornamental plants, and rice (Vurukonda et al., 2018; Lang et al., 2019).

Streptomycin is an effective antibiotic against many bacterial infections because it inhibits translation by binding to the 30s ribosomal subunit, altering its shape and preventing it from binding the 50s subunit, therefore preventing the 70s ribosome from forming (Kornder, 2002). This causes the bacterial cell to generate faulty fatty acids, lipids, and fatty acid derivatives that are essential to forming a functioning cellular membrane (Kornder, 2002). The faulty cell membrane results in the leaking of potassium ions, amino acids, nucleotides, oligonucleotides, and proteins until the cell eventually dies (Kornder, 2002). Streptomycin is only effective against bacteria because eukaryotes have 40s and 60s ribosomal subunits, not 30s and 50s (Klinge et al., 2012). This means that the antibiotic will not damage the plant the bacteria are associated with, but it will be ineffective against fungal pathogens. However, this is not necessarily of concern as *S. griseus* is part of the *Streptomyces* genus and has other mechanisms that can prevent fungal infections.

1.3 How Climate Change Will Affect Plants and Microorganisms

The ability of *S. griseus* to prevent crop diseases can benefit the global economy and food security. However, the climate is changing due to anthropogenic disturbances and it is unclear how this bacterium will respond to these changes (IPCC, 2021). It is also unknown how pathogens will respond to the changing climate (Chakraborty et al., 2011). Weather influences all stages of host and pathogen life cycles, but because pathogens vary with regard to mechanisms of pathogenicity and favor different growth conditions, it is difficult to know on a pathogen- by-pathogen basis how climate change will inhibit or enhance their ability to cause disease in susceptible hosts (Chakraborty et al., 2011).

Table 1. Projected global temperature increases under different IPCC (2021) scenarios

	Near term, 2021–2040		Mid-term, 2041–2060		Long term, 2081–2100	
Scenario	Best estimate (°C)	*Very likely* range (°C)	Best estimate (°C)	*Very likely* range (°C)	Best estimate (°C)	*Very likely* range (°C)
SSP1-1.9	1.5	1.2 to 1.7	1.6	1.2 to 2.0	1.4	1.0 to 1.8
SSP1-2.6	1.5	1.2 to 1.8	1.7	1.3 to 2.2	1.8	1.3 to 2.4
SSP2-4.5	1.5	1.2 to 1.8	2.0	1.6 to 2.5	2.7	2.1 to 3.5
SSP3-7.0	1.5	1.2 to 1.8	2.1	1.7 to 2.6	3.6	2.8 to 4.6
SSP5-8.5	1.6	1.3 to 1.9	2.4	1.9 to 3.0	4.4	3.3 to 5.7

It is believed, however, that climate change will favor pathogens more than plants (Newton et al., 2011). Some aspects of climate change such as increased carbon dioxide concentrations and small temperature increases (around 2 °C) will likely improve crop yields, but these benefits are limited by the fact that global temperature is likely to increase by more than just 2 °C (see Table 1 and Figure 3) (Chakraborty et al., 2011; IPCC, 2021). In certain Intergovernmental Panel on Climate Change (IPCC) (2021) scenarios, temperature increases may stay in the beneficial range above 55° latitude north, but there is limited arable land in these regions so gains in crop yields above 55° latitude north will not make up for the crop losses below this circle of latitude (Newton et al., 2011). However, there is also evidence that elevated carbon dioxide concentrations will increase plant susceptibility to some diseases due to enhanced pathogen fertility, further reducing any potential benefits of increased warming (Newton et al., 2011).

Increasing temperatures are likely to favor pathogens the organisms that carry and transfer a disease (i.e. pathogen vectors), which will in most cases be active earlier in the year because of elevated temperatures (Newton et al., 2011). Additionally, higher temperatures are expected to shorten the time of virus acquisition and the virus's latent period within the host (Newton et al., 2011). This means that plants will not only be exposed to pathogens carried by vectors for a longer period of time, but the pathogen is more likely to be active within the host. As a result, the number and severity of crop diseases, with the possibility for new and emerging diseases, could all arise from climate change (Mahmuti et al., 2009). Changing precipitation patterns are also going to affect crops. Precipitation patterns are not expected to change uniformly across the globe; however, climate models predict that dry places will become more arid and wet regions will receive more precipitation (Trenberth, 2011). The frequency and intensity of droughts in dry areas is going to increase because rising temperatures stimulate evaporation, leading to drier surface conditions (Trenberth, 2011). Additionally, the water holding capacity of air rises by about 7% per degree Celsius increase, making precipitation events in dry areas less likely as the planet gets warmer (Trenberth, 2011). This works the other way in areas that are cooler and more wet. In these regions, the increase in atmospheric water holding capacity causes precipitation events to become more extreme because there is more moisture in the air (Trenberth, 2011).

Drought is problematic for plants because they need water for photosynthesis. Crop fields can be irrigated to make up for a lack of rain, but water is already a limited resource so this could generate a different problem in the future. Excess rain is unsuitable for many crops (e.g. wheat, corn) because it can leach nutrients from the soil and the plant itself, slowing their growth and potentially affecting total yield (Tukey, 1966; Rengel, 2011). Nutrient leaching and waterlogged soil conditions cause plants to deteriorate at an elevated rate (Newton et al., 2011). Excess precipitation also leads to issues with seed sowing and harvesting, directly resulting in crop losses and in some cases shortened growing seasons (Newton et al., 2011). Essentially, weather in the

future is going to become more variable with more extreme events, both of which will negatively impact crop yields (Tubiella, 2007).

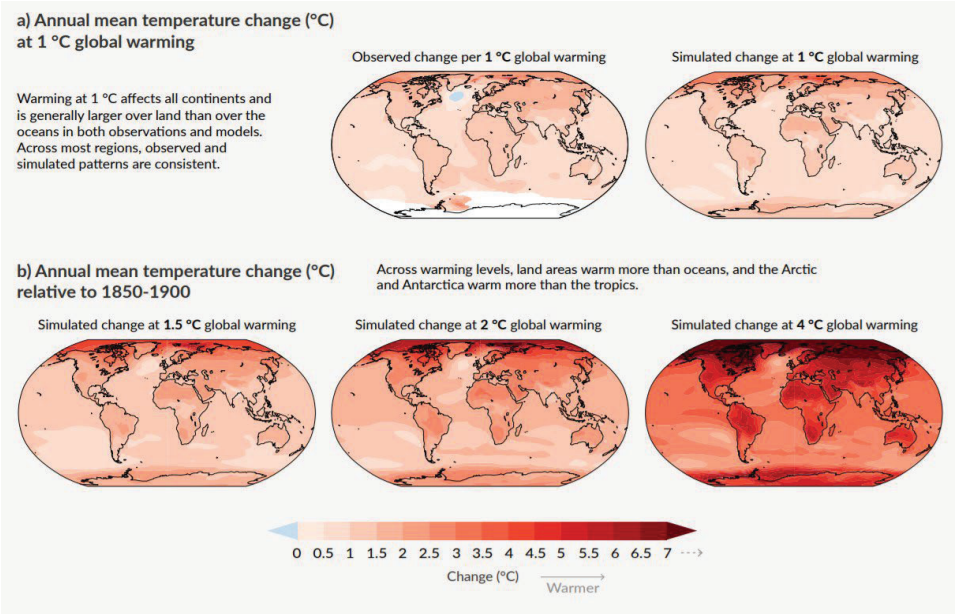

Figure 3. Global heat map of how global temperature changes will affect temperature differences around the world under different IPCC (2021) scenarios.

Beyond crop losses directly caused by drought and excess precipitation, these changing environmental conditions likely favor pathogens over plants. One of the main reasons for this is that pathogens are far more adaptable to environmental stressors than plants are (Newton et al., 2011). Pathogens are also opportunistic and will take advantage of any weakness in a plant's defense systems (Newton et al., 2011). This is foreboding for crops because in addition to the abiotic stressors the plants are expected to encounter, their associated pathogens are likely to be more virulent than before.

S. griseus will not be able to help plants survive changing environmental conditions directly, but by aiding in nutrient acquisition and promoting growth they can help plants better tolerate periods of abiotic stress (Olanrewaju & Babalola, 2019). Given that pathogens are highly adaptable and are likely to become more active in the future, it is important that *S. griseus* remains effective under changing conditions to help keep crop losses to a minimum. However, it is not well understood how *S. griseus* will respond to potential future environmental changes. A better understanding of how *S. griseus* responds to abiotic stressors such as elevated temperatures could help food growers better understand some of the risks their crops will face in the future. If *S. griseus* is unable to respond well to heat stress, farmers can start to strategize how to compensate for the decrease in beneficial rhizosphere productivity to ensure that additional crop losses are kept to a minimum. This could also guide scientists in developing and improving other methods of pest and pathogen control in the event of a decrease in beneficial rhizosphere productivity.

1.4 Metabolomics

1.4.1 Introduction to Metabolomics and Mass Spectrometry

The goal of metabolomics is to characterize an organism's metabolome qualitatively and quantitatively, which can be defined as the collection of all metabolites present in a cell that participate in metabolic reactions and that are required for a cell's maintenance, growth, and normal function (Verpoorte et al., 2008; Dunn & Ellis, 2005). *S. griseus* is well known for producing secondary metabolites and many of the mechanisms by which the bacterium benefits plants are because of secondary metabolite production. Therefore, a powerful method to investigate how changing temperatures will affect *S. griseus's* ability to protect plants from biotic and abiotic stresses is through metabolomics. An organism's metabolome is diverse and contains compounds with a broad range of physical and chemical properties (Dunn & Ellis, 2005).

However, little is known about the size of the *S. griseus* metabolome. However, *Escherichia coli*, which has a genome containing about half as many base pairs as *S. griseus*, is known to produce around 2,600 metabolites (Blattner et al., 1997; Grubbs et al., 2011; Guo et al., 2013). Given this gap in knowledge, it is therefore important to characterize *S. griseus's* metabolome.

Given the wide diversity of metabolites, it is impossible to characterize an entire metabolome using a single technique (Verpoorte et al., 2008). The two primary methods of analyzing a metabolome are nuclear magnetic resonance and mass spectrometry, which will be the focus of this section (Dunn & Ellis, 2005). Mass spectrometry is a technique in analytical chemistry that measures the mass to charge (m/z) ratio of ions present in a sample (Chace et al., 2005). Mass spectrometry is one of the preferred tools for metabolomic analysis because it is a high-throughput approach capable of sensitive and selective qualitative analyses (Dunn & Ellis, 2005).

Mass spectrometers determine the mass of compounds in a sample by forming ions, which can be detected as they are separated in the instrument according to their m/z ratio (Dunn & Ellis, 2005). Before the samples can be injected into a mass spectrometer the analytes must be extracted from the sample. Any given extraction method can only target a certain fraction of the metabolites within a sample, so this must be tailored to the goals of the experiment (Bahureksa et al., 2021). For example, a water extraction will remove a fraction of the polar metabolites in a sample, whereas chloroform will remove a fraction of nonpolar metabolites within a sample. Once the metabolites have been extracted, and cleaned, if necessary, the samples are ready to be injected into a mass spectrometer. The first step in this process is the production of gas phase ions through ionization techniques like electrospray ionization (ESI) (Bahureksa et al., 2021).

ESI is a common ionization method because it generally produces intact ions from the analyte (Bahureksa et al., 2021). Some analytes will still fragment, particularly at high spray voltages, but it is still considered to be one of the "softest" ionization methods available (Bahureksa et al., 2021). In ESI, the sample is converted from a liquid to a fine mist as it is passed through a positively or negatively charged capillary (Bahureksa et al., 2021). In negative mode, ions generally form by deprotonation or by forming adducts with negatively charged ions such as Cl^- (Bahureksa et al., 2021). Inversely, in positive mode, ions form by protonation or by forming adducts with cations such as Na^+, K^+, NH_4^+, or metals (Bahureksa et al., 2021). Between these two ionization modes, a mass spectrometer can detect a wide range of distinct components within a sample (Bahureksa et al., 2021).

A sample's solution chemistry can enhance or reduce the efficiency of electrospray ionization. Hydrophobic solutions generally have greater ESI efficiency than hydrophilic solutions because the affinity for the surface of droplets, where there is a greater probability of molecules being desolvated and charged, is greater (Bahureksa et al., 2021). ESI efficiency is also enhanced when the analytes in solution are already charged, which in the case of basic analytes requires acidic conditions and basic conditions for acidic analytes (Bahureksa et al., 2021). ESI can be suppressed by the presence of contaminants, additives, salts, and metals within the solution by creating matrix effects (Bahureksa et al., 2021).

Another factor that contributes to better experimental results is to increase the magnetic field strength, which will increase the machine's resolution, dynamic range, and reduce the overlap of separate peaks (Bahureksa et al., 2021). Increasing the sample acquisition time can also improve resolution, but if the signals coming from the sample are low this can also result in machine noise being assigned peak values (Bahureksa et al., 2021). Mass spectrometry can provide high accuracy molecular weight assignments for positive and negative metabolites across a wide range of molecular weights, making it a powerful tool in metabolomics, but that does not mean it is without its faults (Verpoorte et al., 2008). The different sensitivities of molecules and differences between ionization techniques and sample matrices can negatively impact the reproducibility of mass spectrometry results (Verpoorte et al., 2008). Fortunately, biological variability is often greater than analytical variability, but these are still issues that have yet to be resolved (Dunn & Ellis, 2005; Verpoorte et al., 2008).

1.4.2 Fourier Transform Ion Cyclotron Resonance Mass Spectrometry (FTICR-MS)

Fourier transform ion cyclotron resonance mass spectrometry (FTICR-MS) and liquid chromatography with tandem mass spectrometry (LC-MS/MS) are the two most commonly used approaches for metabolite characterization. No single method can characterize all the analytes within a sample, but between FTICR-MS and LC-MS/MS a wide range of compounds can be analyzed (Verpoorte et al., 2008).

FTICR-MS is a high throughput approach that allows for high mass resolution analysis of analytes in a sample (Dettmer et al., 2006). Once a sample has been injected into an FTICR-MS and ionized, the ions enter the ICR cell, which is encased within a superconducting magnet (see Figure 4) (Tfaily, 2011). The strength of this magnet will vary by machine with typical ranges between 3 and 14.5 tesla, but the system used for this experiment has a magnetic field strength of 9.4 T (Tfaily, 2011). Once the ions enter the ICR cell, the magnet causes the ion path to bend in a circular motion (Tfaily, 2011). Ions with smaller mass-to-charge ratios will bend more than ions with larger mass-to-charge ratios, allowing ions with different mass-to-charge ratios to be separated, detected, and analyzed separately (Tfaily, 2011).

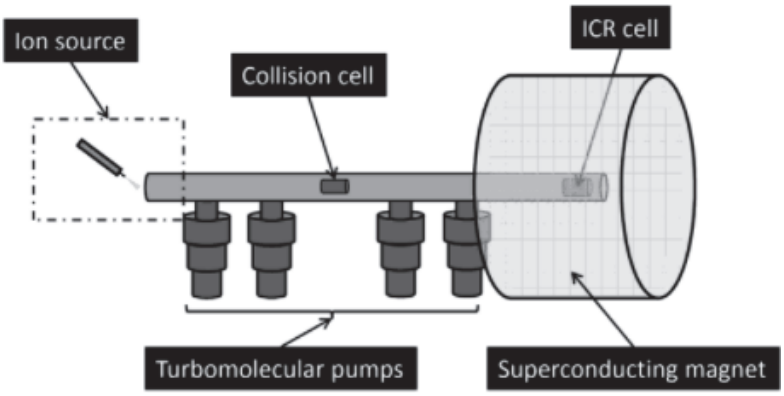

Figure 4. Simplified schematic of a typical FTICR-MS inner components (Tfaily, 2011).

Benefits of FTICR-MS include short analysis times, which improve reproducibility between samples, and mass resolving power of a hundred to several hundred Da, allowing for the precise assignment of molecular formulae to compounds (Dettmer et al., 2006). Despite high resolution and mass accuracy, FTICR-MS is limited in the range of compounds it can detect within a sample. FTICR-MS resolves m/z peaks in the 150-1000 range and has trouble identifying compounds with a mass less than 200 Da (Bahureksa et al., 2021). This can lead to trouble identifying common biological metabolites such as acetate, pyruvate, amino acids, glucose, fructose, and succinate (Bahureksa et al., 2021). However, when paired with other mass spectrometry methods, such as LC-MS/MS, these compounds can be identified (Bahureksa et al., 2021).

Only providing molecular formulae is also a disadvantage of FTICR-MS. The molecular formula is derived from software-based calculations that select a molecular formula with the lowest error or the least number of non-oxygen heteroatoms (Bahureksa et al., 2021). However, this method requires highly accurate mass calibration and can therefore at times result in inaccurate molecular assignments (Bahureksa et al., 2021). Uncertainty with molecular assignments rises significantly with increasing mass and number of elements within the compound because the number of potential formulae increases (Bahureksa et al., 2021). Because the technology is limited to molecular formulae, by itself, FTICR-MS cannot differentiate between isomers, determine molecular structures, or identify functional groups within a compound (Bahureksa et al., 2021).

1.4.3 Liquid Chromatography Tandem Mass Spectrometry (LC-MS/MS)

LC-MS/MS is similar to FTICR-MS, but prior to ionization metabolites are separated by liquid chromatography (Figure 5) (Dunn & Ellis, 2005). Separation between metabolites occurs during chromatography because the metabolites interact with the liquid and mobile phase to different extents, causing them to move between the point of sample introduction and the detector at different rates (Ardrey,

2003). The stronger the molecules in the sample adsorb to the stationary phase, the slower they will move through it (Khan Academy, 2021). The more soluble a molecule is in the mobile phase, the faster those molecules will move through the stationary phase (Khan Academy, 2021). Separation is beneficial for the data because it prevents molecules that would compete for charge if they were introduced at the same time from suppressing the detection of molecules that are ionized less efficiently (Bahureksa et al., 2021). Separation also reduces the number of ions that are present at a time, allowing for the generation of fragmentation spectra for individual compounds, which can be used to resolve structural isomers (Bahureksa et al., 2021). Additional benefits of LC-MS/MS are simplified sample preparation, it requires lower temperatures than other forms of mass spectrometry, and the samples do not need to be suspended in a volatile medium (Dunn & Ellis, 2005).

Chromatographic separation is dependent on the stationary and mobile phase of the column in addition to the chemical characteristics of the sample (Ismail & Nielsen, 2010). As such, it is important that the column is made from materials that will properly interact with the compounds of interest. In untargeted metabolomics, the goal is to extract as many of the metabolites within a sample as possible, so more than one method of chromatographic separation is required (Contrepois et al., 2015).

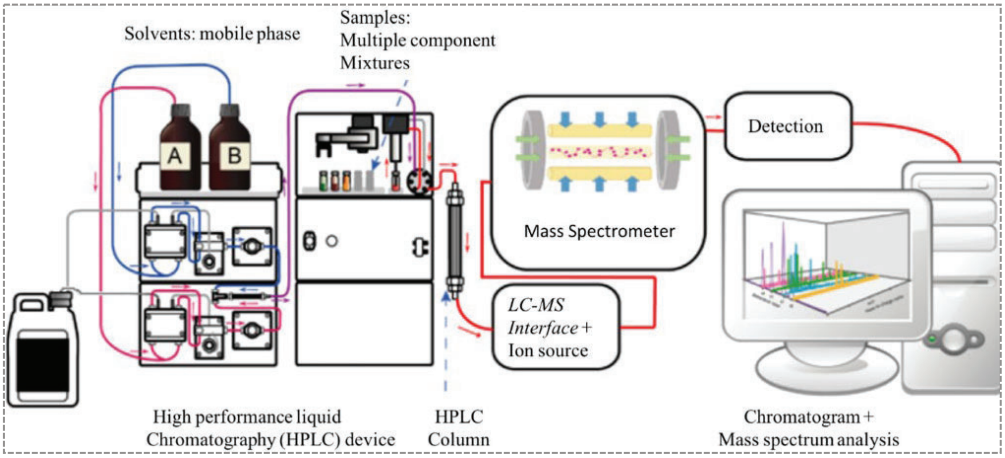

Figure 5. Schematic of LC-MS/MS workflow (Kailasam, 2021).

To characterize non-polar and moderately polar metabolites, the reverse phase (RP) method can be used (Peterson & Cummings, 2005). A RP stationary phase is nonpolar and is primarily made of silica with covalently bound alkyl or aryl functional groups on the surface (Rassi, 2021). This means that nonpolar molecules are going to adsorb to the stationary phase and move through the column more slowly than polar molecules (see Figure 6A). The mobile phase is more polar than the stationary phase, with methanol being one of the most common solvents because its polarity is well suited for RP chromatography, and it ionizes well in mass spectrometers (Rassi, 2021). These solvents can also be mixed with water, which aids in the retention and separation of moderately polar compounds (Rassi, 2021). A moderately polar mobile phase means that moderately polar molecules that are more soluble will move through the column faster than nonpolar molecules that are less soluble. However, even with water additions, RP is not fit for characterizing strongly polar compounds such as amino acids, organic acids, sulfates, and sugars because they are soluble in the mobile phase and do not interact strongly with the stationary phase, meaning they move through the column quickly and enter the mass spectrometer in quick succession. Because RP chromatography targets primarily nonpolar metabolites, to characterize the widest range of metabolites it is important to use another separation method such as hydrophilic interaction chromatography (HILIC) that will effectively separate polar metabolites (Contrepois et al., 2015).

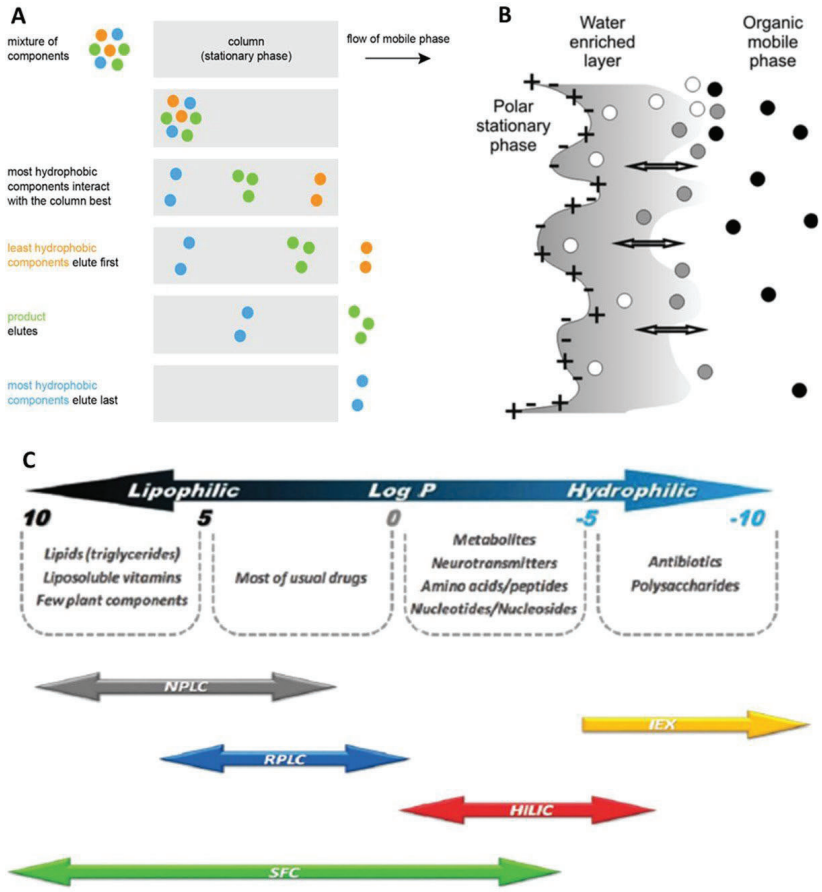

Figure 6. (A) Reverse phase chromatography (Creative Biostructure, 2022). (B) Schematic of compounds moving through a HILIC system (white dots = hydrophilic, gray dots = semi-hydrophilic, black dots = hydrophobic) (Jensen et al., 2012), (C) Metabolite coverage of different chromatography techniques (Guillarme & Veuthey, 2017).

For HILIC, any polar stationary phase can be used, but typical surfaces are made up of silica and some may have polar functional groups attached to the surface (Buszewski & Noga, 2012). This polar surface means that polar molecules will strongly adsorb to the stationary phase and will move through the column slower than nonpolar molecules (Figure 6B). A HILIC mobile phase is also polar and generally consists of an organic acid such as acetonitrile mixed with water, a combination that ionizes well and is therefore compatible with mass spectrometry (Buszewski & Noga, 2012). A moderately polar mobile phase means that polar molecules are more soluble than nonpolar molecules and will move through the column faster. Because HILIC separates polar metabolites, it is a complementary approach to RP and the two combined greatly expand the coverage of a sample's metabolic profile (Figure 6C) (Contrepois et al., 2015; Guillarme & Veuthey, 2017). HILIC is additionally capable of separating some charged substances, a role typically reserved for ion exchange chromatography (Buszewski & Noga, 2012).

Chapter 2: Assessing the Effect of Temperature on the Growth and Metabolite Production of *Streptomyces griseus*

2.1 Introduction

In 2020, one third of the world's population did not have adequate access to food (UN, 2021). Given that the global population is expected to increase by two billion over the next 30 years, it is important that gains in food production are made in the near future (UN, 2019; Mahmuti et al., 2009). However, increasing agricultural production is not a simple task. Currently a significant amount of the Earth's terrestrial surface is devoted to agriculture (~ 40%). Thus, any significant future gains in agriculture forced by the increase in the population number will likely need to come from improving current practices, and not necessarily from expanding farmland (FAO, 2003). Furthermore, 20 to 40% of all crops produced on the Earth's terrestrial surface are lost to pests (e.g., insects and pathogens), per the Food and Agriculture Organization (2019). Annually, pathogens cause $220 billion in losses while insects result in $70 billion in losses (FAO, 2019).

There are multiple ways by which crop losses due to disease can be minimized, including the use of pesticides and other agrochemicals, genetically modifying plants for resistance to specific diseases, selectively breeding for plants that have acquired immunity to a pathogen, and promoting beneficial rhizosphere activity (Lugtenberg & Kamilova, 2009). All these options have potential, and are probably most effective in conjunction with one another, but they all have disadvantages too. Genetically modifying plants and the use of pesticides are unpopular with consumers and governments, making their use limited for now (Lugtenberg & Kamilova, 2009). Pesticides are unpopular because they leave behind chemical residues on crops that are potentially toxic to the environment, and they drive up the cost of production (Krishna & Qaim, 2008). Genetically modified crops are unpopular primarily due to a lack of education on the topic (Wunderlich & Gatto, 2015). Studies have shown that people who are more educated on the science of genetically modified organisms are more accepting of them than people who are less educated on the topic (Wunderlich & Gatto, 2015). Consumers who are less knowledgeable on the topic often hold false beliefs about how genetically modified crops are made and what they mean for consumer health, often leading to negative perceptions such as genetically modified foods being dangerous to eat (Wunderlich & Gatto, 2015). Genetically modifying and selectively breeding plants generally takes a long time and can result in only short periods of pathogen resistance, which is problematic considering the speed in which agriculture must be scaled up (Lugtenberg & Kamilova, 2009). Another source of pathogen control comes from the soil surrounding plant roots, the rhizosphere. The rhizosphere contains microbes beneficial to plant growth and protection, but if the activity of beneficial bacteria is reduced because of changing environmental conditions, crops could become less resilient to diseases (Mendes et al., 2013).

One particular organism of interest that lives in the rhizosphere is *Streptomyces griseus*. *S. griseus* protects plants from pathogens and promotes growth by producing antibiotics, enzymes, siderophores, volatile organic compounds (VOCs), plant growth regulators, spores, and hyphae (Mendes et al., 2013; Olanrewaju & Babalola, 2019). *S. griseus* is present in soils throughout the world and plays an important role in plant health (Mendes et al., 2013; Sottorf et al., 2019). However, it is unknown how *S. griseus's* metabolism will respond to changing environmental conditions such as global warming. Previous work has investigated the metabolomics of *S. griseus* at a single temperature or looked at the effect of elevated temperature on the streptomycin producing gene, but despite an extensive literature search, we could not find any studies comparing the metabolomic profile of *S. griseus* at different temperatures (Shinkawa et al., 1991; Ohnishi et al., 2003; Sottorf et al., 2019; Youn et al., 2015).

Per the Intergovernmental Panel on Climate Change (IPCC) (2021), global mean surface temperatures will continue to increase until at least the mid-century, with predictions of a 1.5 ˚C global increase in the best case and 4.5 ˚C in the worst case (Figure 7). Small temperature increases, such as those around 2 ˚C, are expected to help crop growth in areas above 55˚ latitude north, but the benefits would be limited given the small amount of arable land in this area and the losses that would also be expected below 55˚ latitude north (Chakraborty et al., 2011; Newton et al., 2011). Rising temperatures are expected to

dampen crop yields by creating environments that are no longer ideal for crop growth and by increasing plant susceptibility to pathogens (Newton et al., 2011). It is generally assumed that rising temperatures will increase the activity of pathogens as a whole, but on a per disease basis, climate change may inhibit, enhance, or have no effect on a given disease's pathogenicity (Newton et al., 2011). Since *S. griseus* is capable of protecting plants from different diseases, it is important to know how these capabilities may be affected given the need to reduce crop death given exposure to pathogens that may become more virulent in addition to the myriad of other side effects of climate change that are unfavorable for crop growth.

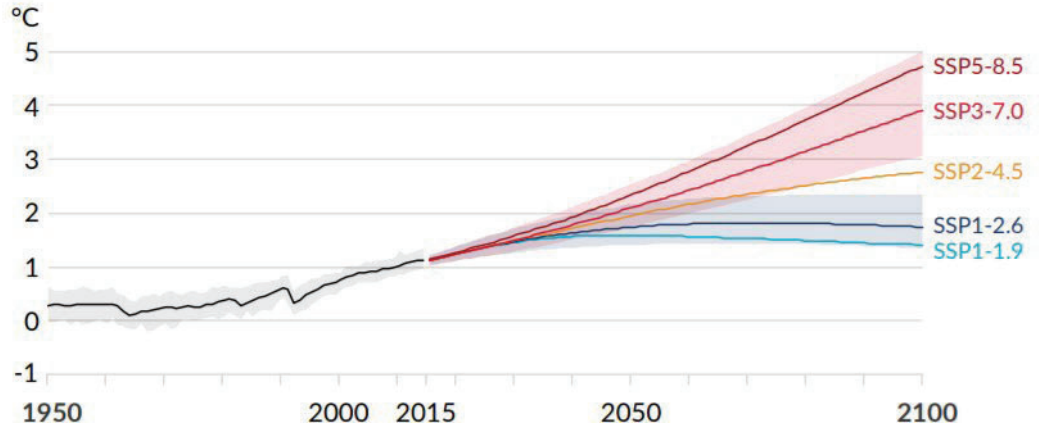

Figure 7. Predicted global warming through the year 2100 based on different IPCC (2021) scenarios. The x-axis represents the year and the y-axis represents the increase in average global temperature since 1950.

Because *S. griseus* produces a wide range of metabolites that affect plant growth and resilience, the question of how temperature affects metabolite production was investigated via metabolomics. The goal of metabolomics is to characterize an organism's metabolome qualitatively and quantitatively, which can be defined as the collection of all metabolites present in a cell that participate in metabolic reactions and that are required for a cell's maintenance, growth, and normal function (Verpoorte et al., 2008; Dunn & Ellis, 2005). It is impossible to characterize an organism's entire metabolome through one method, but to gather as much relevant metabolomic data as possible this experiment utilized an untargeted approach using a combination of Fourier transform ion cyclotron resonance mass spectrometry (FTICR-MS) and liquid chromatography with tandem mass spectrometry (LC-MS/MS) (Verpoorte et al., 2008). Even though these two approaches cannot analyze the whole metabolome, together they generate an abundance of data and characterize a wide range of compounds, making it a relatively unbiased approach (Verpoorte et al., 2008).

Given the gap in research, the objective of this experiment is to determine how *S. griseus* changes its metabolism in response to extreme temperatures. The information gained from this study will further understanding of the potential impacts global warming could have on *S. griseus's* role in crop growth and protection. Previous studies have investigated the effect of elevated temperature on streptomycin production in *S. griseus*. Shinkawa et al. (1991) and Deeble et al. (1995) found that when incubated between 34-36 ℃, *S. griseus* lost resistance to streptomycin and stopped producing the compound. Additionally, Suutari and Laasko (1992) found that fatty acids with the same precursors as many antibiotics in *S. griseus* were produced in the greatest amount in a range between 20-26 ℃, suggesting peak antibiotic production in this temperature range. These are the current extent of studies investigating how *S. griseus* responds to elevated temperatures. The majority of studies incubated *S. griseus* at 28 ℃ and did not compare results across different temperatures (Ohnishi et al., 2003; Sottorf et al., 2019; Youn et al., 2015; Laxman & More, 2002)

For this study, it was hypothesized that *S. griseus* would grow optimally at 22 ℃ with limited growth at 4 ℃ and 35 ℃. Bulk metabolite production is expected to be approximately proportional to growth, with the greatest metabolite production and diversity at 22℃. By analyzing the metabolites produced by *S. griseus* under different temperature conditions inferences can be made to predict how climate change will affect this organism's metabolism, and in turn how this may affect crops in symbiosis

with *S. griseus*. This knowledge will be valuable in preparing for a future in which climatic conditions will be non-ideal for crop production despite the need for an increase in production.

2.2 Materials and Methods

2.2.1 Inoculation

Both solid and liquid media were prepared using tryptic soy powder from Beckton, Dickinson, and Company (REF: 211822, LOT: 0070953). Solid media was prepared by adding 15 grams of powder and 7.5 grams of agar crystals from Fisher Scientific (REF: BP1423-500, LOT: 196854) to 500 milliliters (mL) of deionized water. The mixture was then homogenized by swirling the bottle by hand and then placed into an autoclave where it was sterilized by the Liq20 setting (i.e. 20 minutes under slow exhaust conditions). Once the bottle of media was sufficiently cool to handle without hot gloves, roughly 25 mL of tryptic soy agar was poured into each Petri plate and 10 mL of tryptic soy broth was pipetted into each 20 mL plastic vial in a biosafety cabinet pre-treated with UV light for 15 minutes. Preparation of liquid media followed the steps above, using the same powder-to-water ratio, but no agar was added.

Once both types of media had cooled to room temperature, they were ready for inoculation with *S. griseus* (Figure 8). Eighteen vials of liquid media were made, fifteen were inoculated by swabbing an isolated colony from a previously prepared solid plate with an isolated culture of *S. griseus* then swirling the inoculating loop in the liquid media. The plate used to provide bacteria for the liquid vials was created using a pure culture swab of *Streptomyces griseus* subspecies *griseus* derived from ATCC 10137 from Microbiologics (REF: 0859K, LOT: 859-38-4) to inoculate five plates using a three-section streak to isolate method which were then grown statically at 22 ± .2 ˚C for one week. A different isolated colony was used for each liquid culture inoculation because the colony was destroyed when swabbed with the loop. Eighteen plates of solid media were made and fifteen of those were inoculated by pipetting and then spreading 100 µL of a 10^{-3} dilution of a previously prepared liquid media inoculated with one colony of *S. griseus* that had been growing statically with daily mixing by hand at 22 ± .2 ˚C for a week. The 10^{-3} dilution factor was previously determined to yield the best results after performing plating tests with serial dilutions ranging from 10^{0}-10^{-5}. Solid plates were wrapped in Parafilm from Bemis after inoculation to reduce the risk of post-inoculation contamination. A visual representation of this procedure is shown in Figure 8.

Three plates and three vials of media were prepared but not inoculated to serve as negative controls. Preparation of the controls followed the exact procedure as the inoculated cultures except that the inoculation loop was spread on/through the media after flaming without transferring bacteria. This was done to ensure that in addition to the media, the method used to transfer bacteria to fresh media was sterile. One control of liquid media and solid media were incubated in each temperature zone to verify there was nothing in the environment that would contaminate the plates.

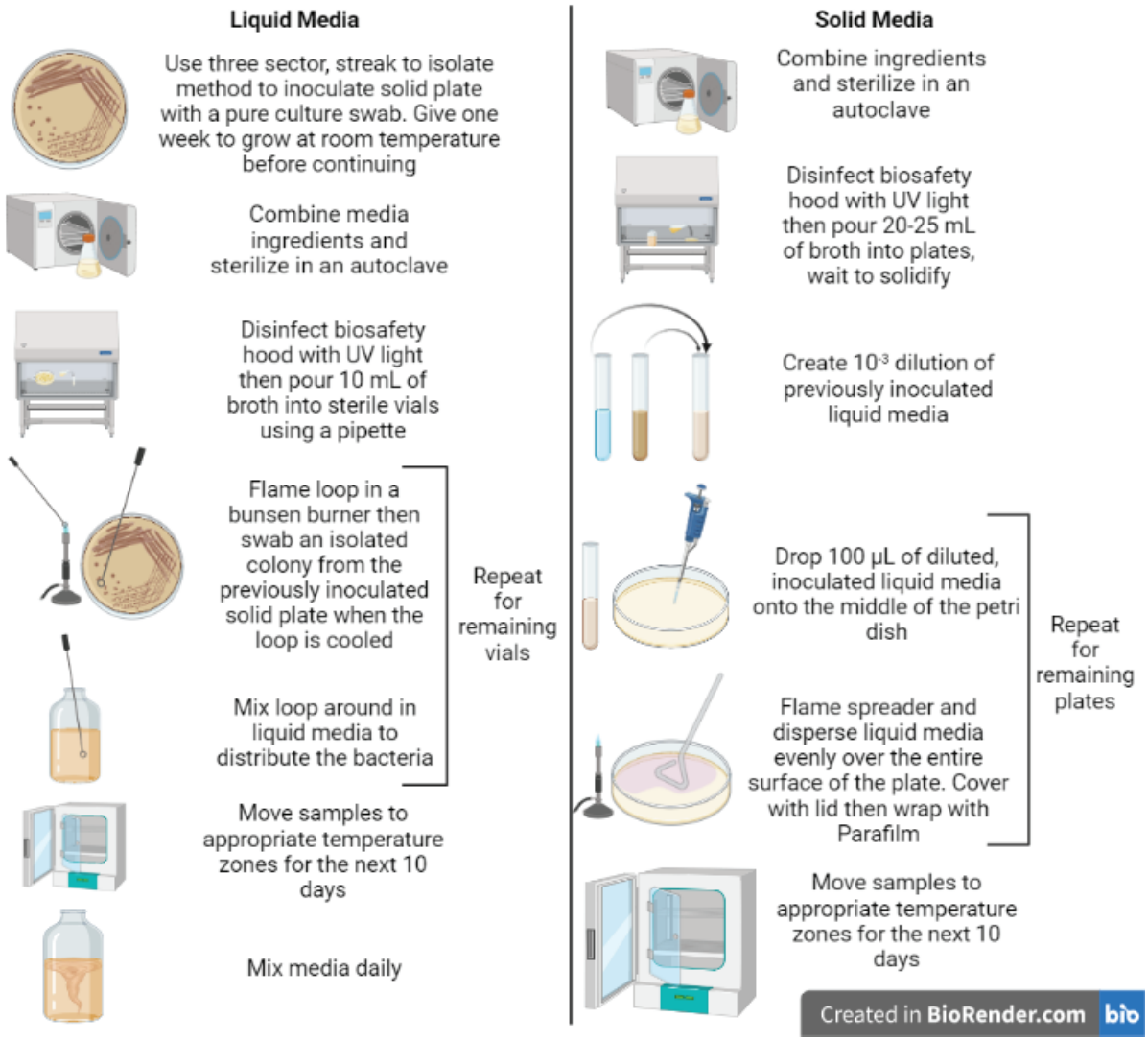

Figure 8. Overview of liquid and solid media inoculation procedures.

2.2.2 Incubation Set-up

Immediately after the plates and vials were inoculated, they were moved to their respective incubation zones. This experiment had three temperature treatments: 4 ± .2 ˚C, 22 ± .2 ˚C, and 35 ± 1˚C. Solid and liquid cultures were distributed evenly between the temperature zones, with 5 inoculated samples and 1 blank of each media type in each temperature zone. Samples were incubated at 4 ˚C in a multi-lab walk-in refrigerator, 22 ˚C samples were stored in a climate-controlled room, and 35 ˚C samples were kept within a Boekel Scientific (Bucks County, PA) incubator. Liquid samples were stirred daily to prevent clumping by gently swirling the vial by hand for 10 seconds. Liquid samples were briefly removed from their incubation zones each day to extract a small amount of sample for absorbance readings. Solid samples spent 10 days incubating before they were permanently removed and prepared for FTICR-MS and LC-MS/MS.

2.2.3 Growth Curve Data Collection and Analysis

To construct a growth curve for the bacteria in each temperature zone, absorbance measurements were taken using a BioTek (Winooski, VT) Synergy H1 microplate reader every 24 ± 2 hours for 10 days. Each day, 200 µL of inoculated media were removed from each vial of liquid media using sterile pipette tips and transferred to one of 18 wells in a clear 96 well plate (Figure 9). The transfer was done in a biosafety cabinet pre-treated with UV light for 15 minutes. The absorbance of each full well was measured at an optical density of 600 nm. In an attempt to reduce the effect of machine variability in the data, each plate was tested three times in immediate succession. A visual representation of this procedure can be seen in Figure 9.

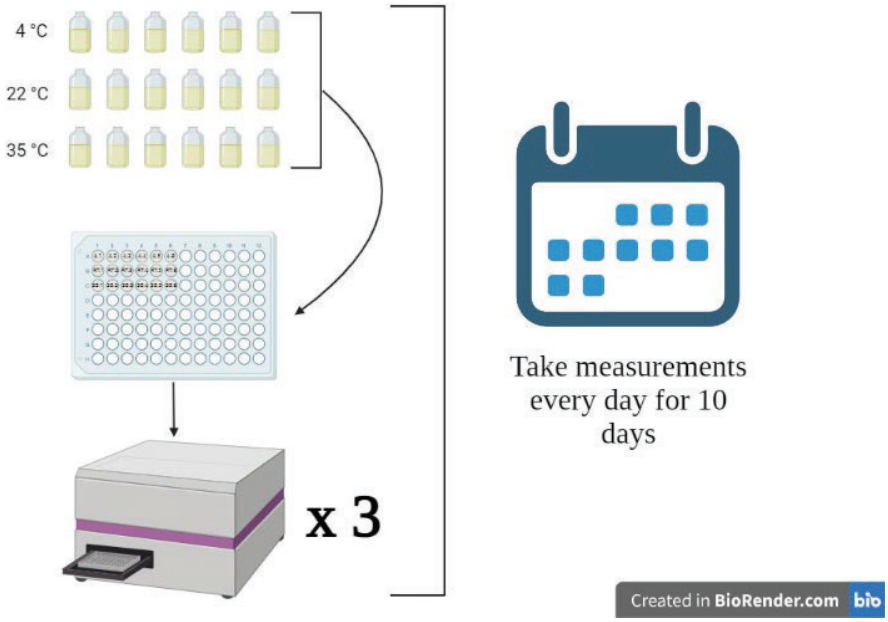

Figure 9. Visualization of growth curve data collection procedure.

Absorbance data was exported to and processed in Excel. First, the absorbance of each well across the three runs was averaged to reduce the effect of machine variability. The average absorbance and standard deviation for each temperature treatment per day, with the exception of the blanks, was then calculated using the average from each individual well in each temperature treatment each day. The average absorbance for each temperature for each day was then plotted on a plot of absorbance versus time using R (Figure 14).

2.2.4 FTICR-MS Data Collection and Analysis

Samples for FTICR-MS and LC-MS/MS were taken from the solid Petri plates in the form of agar disks (Figure 10). To collect the disks, the heads of sterile 15 mL falcon tubes were pressed into the media in approximately the same spots for each plate. Disks were taken in similar spots in each plate instead of selecting for areas with high bacterial density to reduce sampling bias. The tube cut into the agar, forming circular disks that could be stored in the tube used to cut it out. Two disks were taken from each plate and stored in the same tube. The disks were then freeze dried at -50 ˚C for 48 hours in a Labconco (Kansas City, MO) freeze dryer, which removed all moisture from the disks and made them brittle. After 48 hours the disks were brittle and removed from the freeze drier. Immediately after removal the disks were beaten into a powder using BioSpec Products' (Bartlesville, OK) Mini- beadbeater. Once in powder form, the samples were

suspended in an 80:20 solution of methanol (80%) and deionized water (20%). The samples were then centrifuged at 7800 RPM for 10 minutes, separating the supernatant from the pellet. The supernatant was split evenly between two falcon tubes, with one tube going towards FTICR-MS and the other towards LC-MS. See Figure 10 for a visual representation of this procedure. The vials were stored at – 80 ˚C until they were further processed for FTICR-MS and LC-MS/MS.

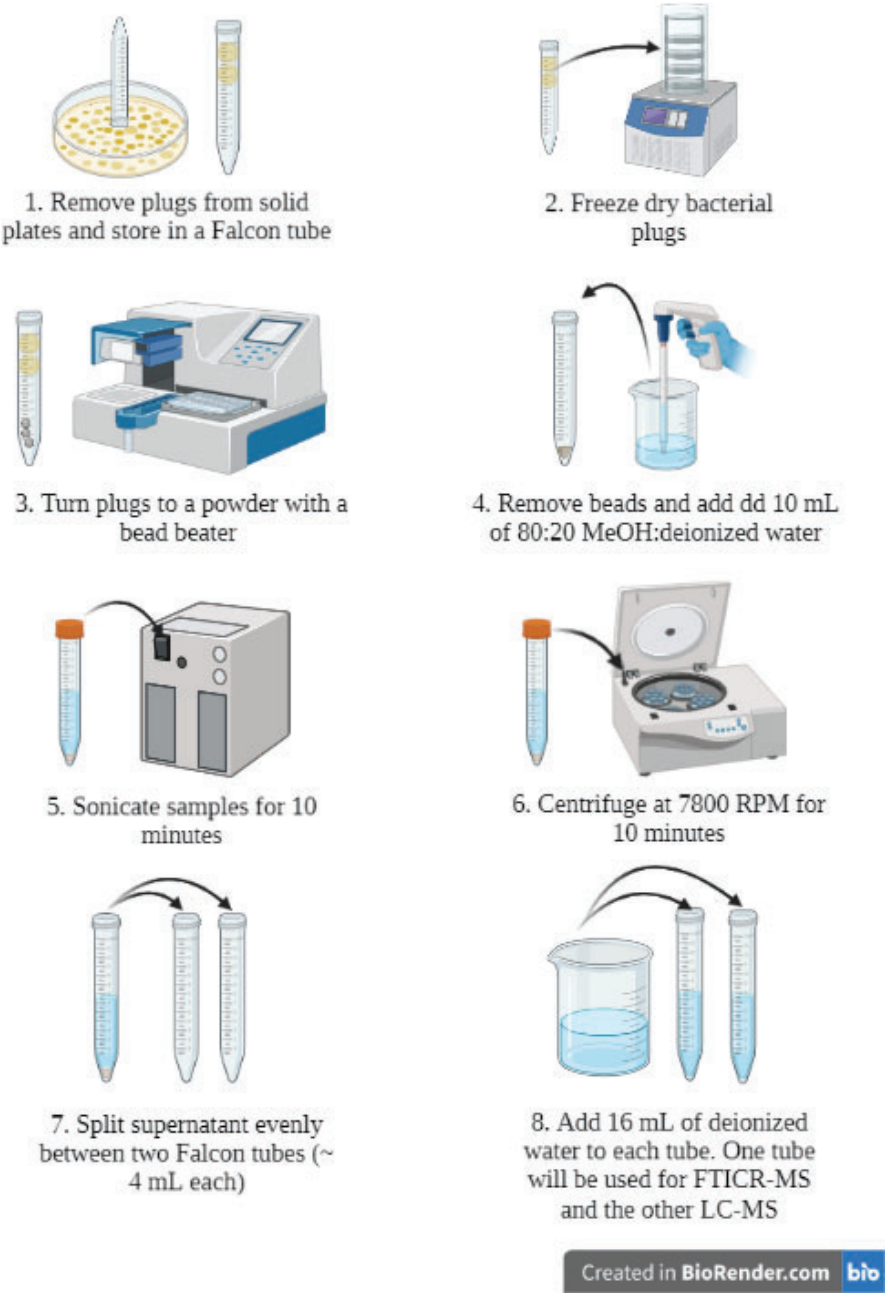

Figure 10. Overview of the bacterial plug collection and preparation procedure.

The samples that were set aside for FTICR-MS were further processed through solid phase extraction (SPE), a process that concentrates metabolites and removes excess salts, prior to injection into the mass spectrometer (Figure 11). SPE first involves acidifying the sample to a pH between 2 and 3 which protonates acidic functional groups, decreases polarity, and improves stationary phase binding (Bahureksa et al., 2021).

After acidification, the sample is run through a column that contains nonpolar material and acidic functional groups, which retains metabolites but not salts (Bahureksa et al., 2021). The columns were then air dried and eluted with methanol, which carries the metabolites through the column into a vial. At this point, the samples are ready for direct injection into the mass spectrometer. See Figure 11 for a visual representation of this procedure.

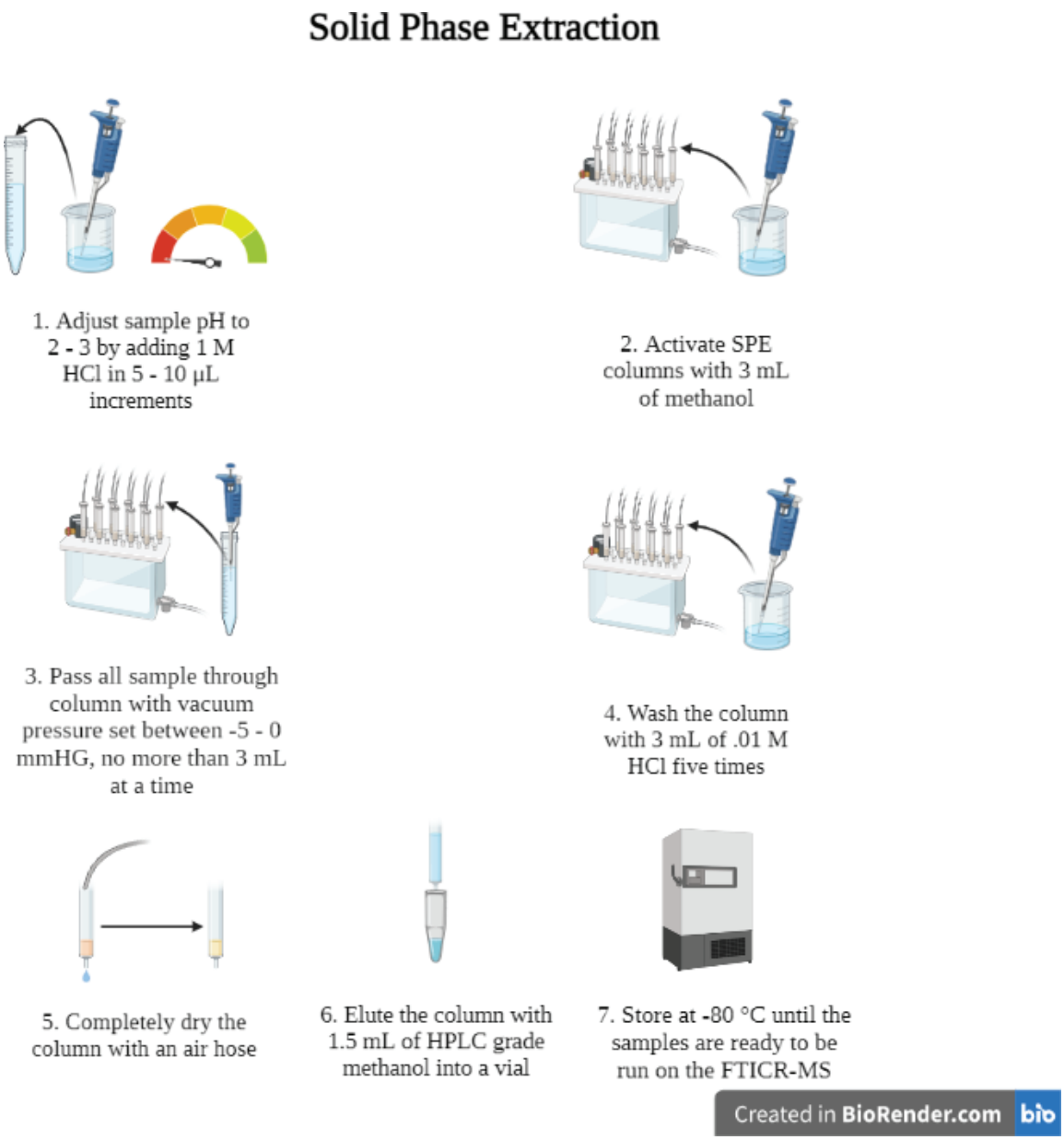

Figure 11. Visual representation of the steps for solid phase extraction, the procedure done to prepare samples for FTICR-MS

Mass spectra were collected by direct injection into a 9.4 tesla Bruker (Billerica, MA) FTICR mass spectrometer. Before any samples were injected, the injection line was flushed five times with HPLC grade methanol to remove any contaminants or metabolites present in the line from previous experiments. To ensure the line was clean and that the instrument is functioning properly, both a methanol blank and a Suwannee River Fulvic Acid (SRFA) control were run first. 144 scans were collected for each sample in negative ion mode with an accumulation time of .02 seconds. Between each sample the line was flushed

with methanol 3-5 times while the machine was on tuning mode to guarantee there were no remaining peaks from the previous sample. Once the raw spectra were generated, peaks were first picked then calibrated using the software Compass DataAnalysis 4.2 from Bruker using the following parameters: signal to noise ratio > 7, calibration group = ESI, mode = linear, search range = .005, intensity threshold = 1,000,000. Once calibrated, molecular formulae were assigned to the m/z ratios using the software Formularity (Tolić et al., 2017).

To visualize the data, a report file from Formularity and a custom metadata file were run in Metabodirect, a hybrid R and Python FTICR-MS data visualization pipeline that was developed in the Tfaily Lab (Ayala, 2021). This program was used to generate Figures 15-18. In Figure 16, the compound classes were determined using a Van Krevelen (VK) diagram. In a VK diagram, the O:C and H:C ratio of every identified molecular formula is plotted on the X and Y-axis, respectively (Tfaily, 2011). Biomolecule classes have characteristic O:C and H:C ratios, causing them to cluster in specific regions when plotted, which allows for simple class identification (Tfaily, 2011). In Figure 17, Gibbs free energy (GFE) was calculated using the nominal oxidation state of carbon (NOSC), which is a measure of the energy required to oxidize the carbon in every compound and can be calculated from a compound's molecular formula (AminiTabrizi et al., 2020). When GFE is negative, reactions are exergonic, meaning they occur spontaneously and produce energy. When GFE is positive, reactions are endergonic, meaning they required an input of energy to proceed. Figure 18A visualizes the aromaticity index. Aromaticity index is a measure of the density of carbon-carbon double bonds in a compound (Koch & Dittmar, 2006). Figure 18B visualizes double bond equivalence (DBE), which is a measure of the number of H_2 molecules that would need to be added to a compound to convert all pi bonds to single bonds and all aromatic compounds to acyclic structures (UCLA, n.d.). Higher DBE means more H_2 molecules would need to be added than at lower DBE.

2.2.5 LC-MS/MS Data Collection and Analysis

Samples for LC-MS/MS were collected and initially prepared in the same manner as those for FTICR-MS, but after the supernatant was divided, the methods diverged (see first paragraph section 2.2.4 and Figure 10). For LC-MS/MS samples, the supernatant was split evenly between two 2 mL vials and dried in an Eppendorf (Hamburg, Germany) Vacufuge plus, leaving behind a small pellet. The pellet was stored in a -80 ˚C freezer until there was availability on the 9.4 tesla Bruker mass spectrometer for LC-MS/MS. Two days prior to the time of LC-MS/MS data collection, the samples were removed from the -80 ˚C freezer and suspended in 500 µL of the first reconstitution solution, an 80:20 mix of deionized water (80%) and HPLC grade methanol (20%). After resuspension, the samples were stored at 4 ˚C overnight.

The following day, half of the sample was removed from each tube and transferred into new tubes. These new tubes were ready for half of the LC-MS/MS process, reverse phase (RP), but the other half in the original tubes required further preparation. These tubes, which were to be prepared for hydrophilic interaction chromatography (HILIC), were completely dried in the Eppendorf Vacufuge plus, as they were before. Once dry, the pellets were suspended in a 50:50 solution of deionized water and acetonitrile, finalizing the preparation for HILIC analysis. A quality control tube was prepared for both RP and HILIC samples by combining 5 µL of each sample into a single test tube. Additionally, blanks were prepared for RP and HILIC analysis by filling a 2 mL tube with the appropriate reconstitution solution. See Figure 12 for a visual representation of this procedure.

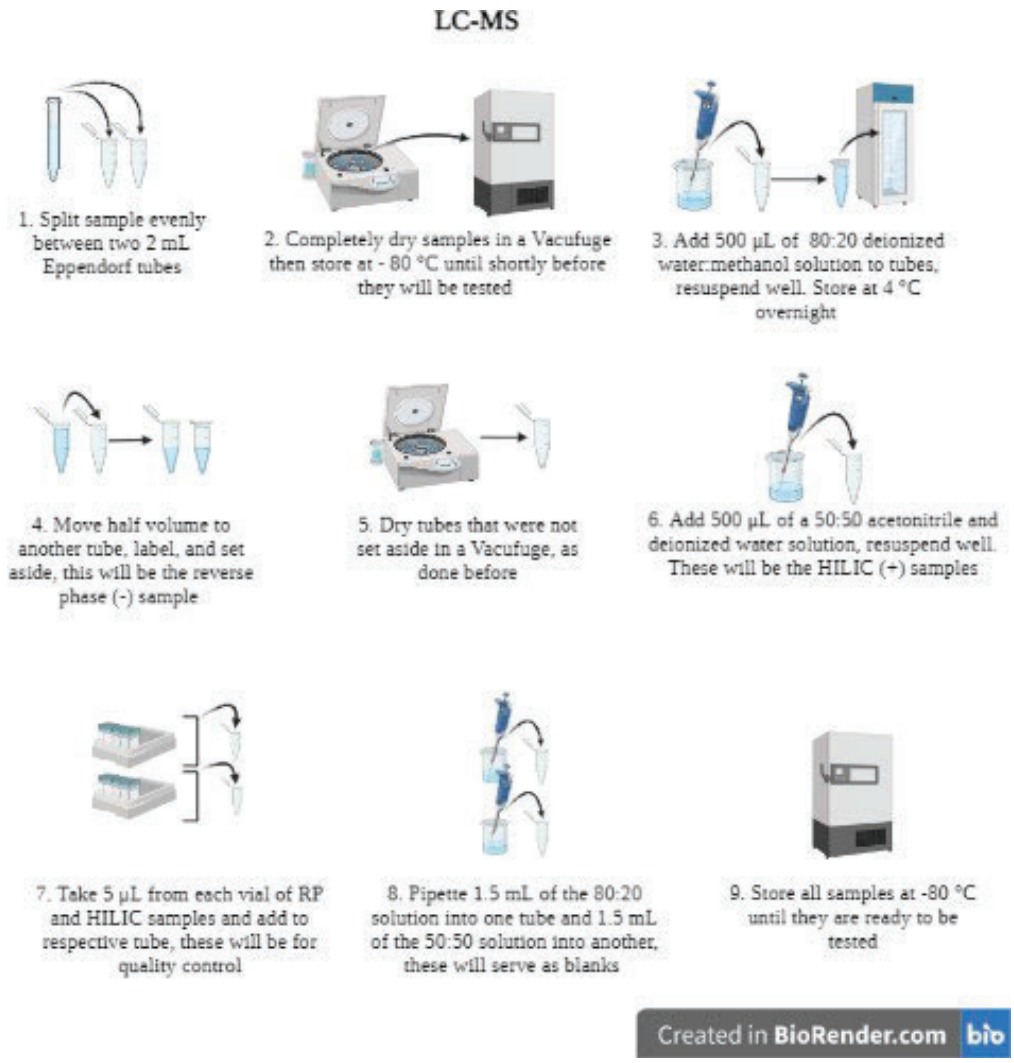

Figure 12. Sample preparation for LC-MS

Raw LC MS/MS data were processed in Compound Discoverer 3.2 software from Thermo Fisher Scientific (Waltham, MA). Compound Discoverer output .csv files containing data on compound name, molecular weight, molecular formula, and peak intensity. The output files were put into Metaboanalyst 5.0, a free online metabolomics data processing website that uses R to create a variety of figures. Because many of the compounds annotated by Compound Discoverer were not assigned a compound name, a second set of .csv files containing only masses with compound names were included. Before figures were made, the data was normalized in Metaboanalyst by normalizing by sum, log transforming, and centering by mean. The files containing only features with compound names were used to construct volcano plots (Figures 22A and 22B), but figures 20 and 21 were made using all available data. The top 50 features from each volcano plot were searched in PubChem, ChEBI, and the University of Arizona Library database to find a function associated with the compound. Compounds that were not recognized in any database, were known to exist but did not have functional information or appeared to be misassigned were used to construct a Van Krevelen diagram to understand the class of compounds they belong to (Figure 22C). Volcano plots are coordinate maps of data points defined by the point's effect size and statistical significance (Goedhart & Luijsterberg, 2020). In Figures 22A and 22B, the characteristic volcano shape shows which compounds are up and down regulated at 35 ˚C relative to at 22 ˚C.

2.3 Results

2.3.1 Solid Culture Microbial Growth

The total growth of bacteria on the solid plates after a ten-day incubation period can be seen in Figure 13. Bacteria incubated at 4 ℃ did not show any growth, whereas bacteria incubated at 22 ℃ grew in distinct colonies on every inoculated plate, and finally the bacteria incubated at 35 ℃ grew, but inconsistently. Two of the 35 ℃ plates grew in an abundant lawn morphology resembling a biofilm, whereas the other two plates grew in a sparse lawn morphology on the edges of the plates, and finally, one plate grew two distinct but small colonies.

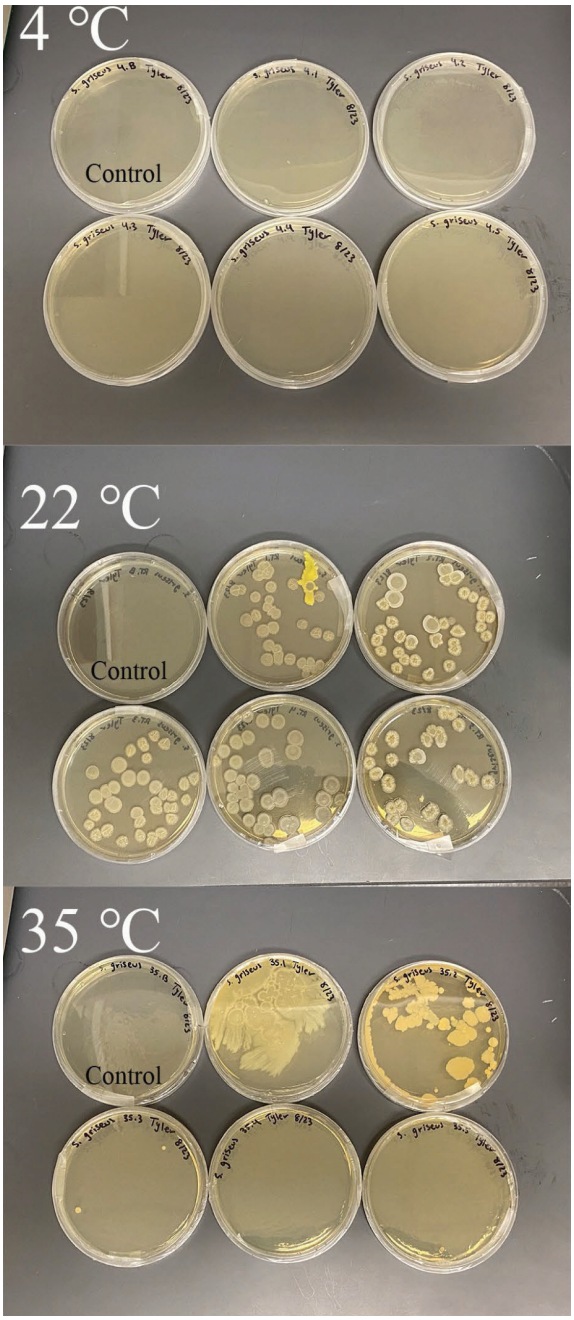

Figure 13. *S. griseus* growth on tryptic soy agar after 10 days of incubation at 4 ℃, 22 ℃, and 35 ℃.

2.3.2 Liquid Culture-Based Microbial Growth Curve

Figure 14 shows the growth curve of *S. griseus* grown in liquid media at each temperature constructed from 600 nm absorbance measurements taken daily over a 10-day period shows a similar trend to the growth patterns in Figure 13. Bacteria grew in the greatest abundance and at the greatest rate at 22 ℃. Bacteria incubated at 35 ℃ grew in the second greatest abundance, but at a much lower level and at a slower rate than the bacteria at 22 ℃. Bacteria incubated at 4 ℃ did not show any growth. The increasing error bars over time can be attributed to variable growth among the samples and issues with clumping in some samples but not others.

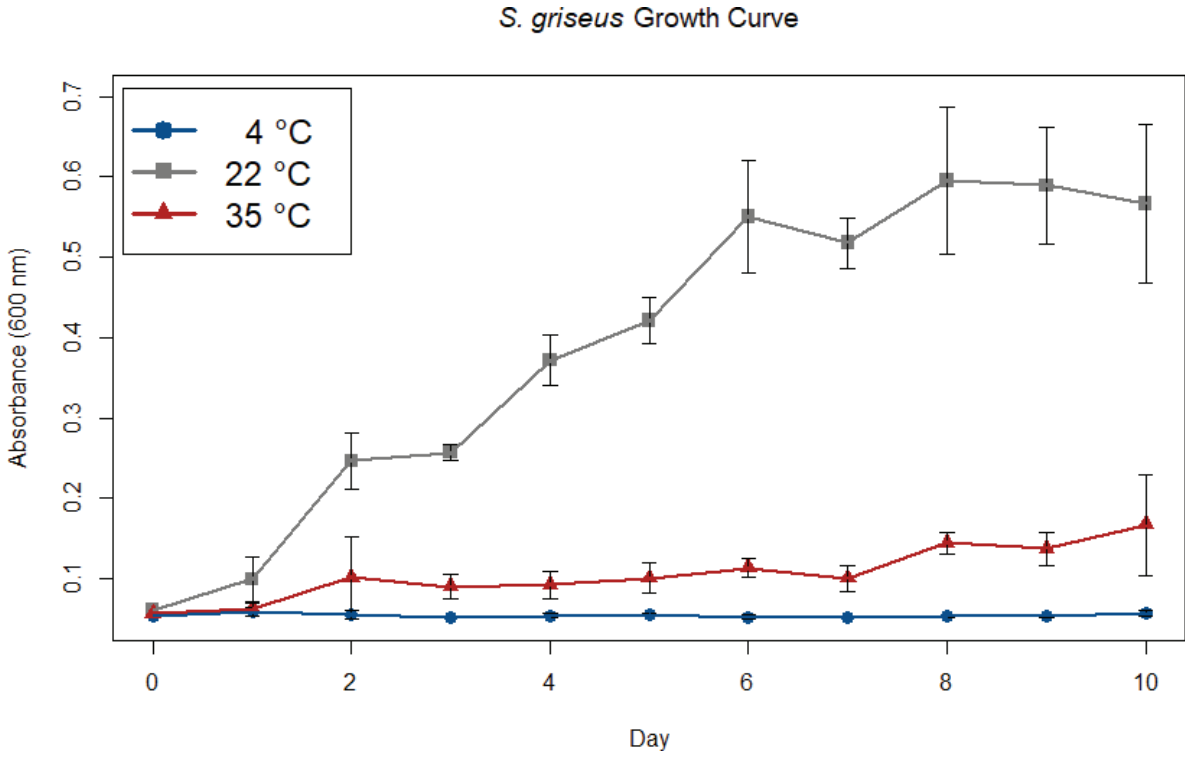

Figure 14. Growth curve of *S. griseus* at different temperatures based on 600 nm absorbance data taken over a 10-day period

2.3.3 Metabolomics Data as Inferred from FTICR-MS

Principal component analysis (PCA) of data generated by FTICR-MS revealed differences in compound class, composition, and abundance between the different temperature treatments and control samples. PC1 and PC2 explained almost 100 % of the variation in organic matter composition between the different samples. The vector arrows show which compound classes are driving the differences in relation to each PC, with the intensity of the vector describing how strongly that class drives the difference. Figure 15 shows strong clustering of the 22 ℃ samples, showing those samples contained compound class profiles similar to each other but different from the other temperature treatments and controls. Differences at 22 ℃ were primarily driven by changes in protein-, condensed hydrocarbon-, carbohydrate-, and lipid- like compounds. Points relating to samples incubated at 4 ℃, 35 ℃, and the controls are dispersed and intermixed, with differences primarily driven by lignin-like or phenolic compounds, unsaturated hydrocarbons, and lipids.

PCA plots are an initial tool used to look for differences between samples to help guide further analysis, so conclusions about the samples cannot be directly gleaned from Figure 15. Figure 16 is

similar in this regard. The bars in Figure 16 represent the relative proportion of different compound classes present in each sample, with the total adding up to 100%. At 22 ℃, we observed a decrease in the abundance of unsaturated hydrocarbons and an increase in the abundance of proteins, condensed hydrocarbons, and carbohydrates relative to the controls. At 4 ℃ and 35 ℃ there was an increase in lignin-like or phenolic compounds and a decrease in lipids relative to the 22 ℃ samples and the controls.

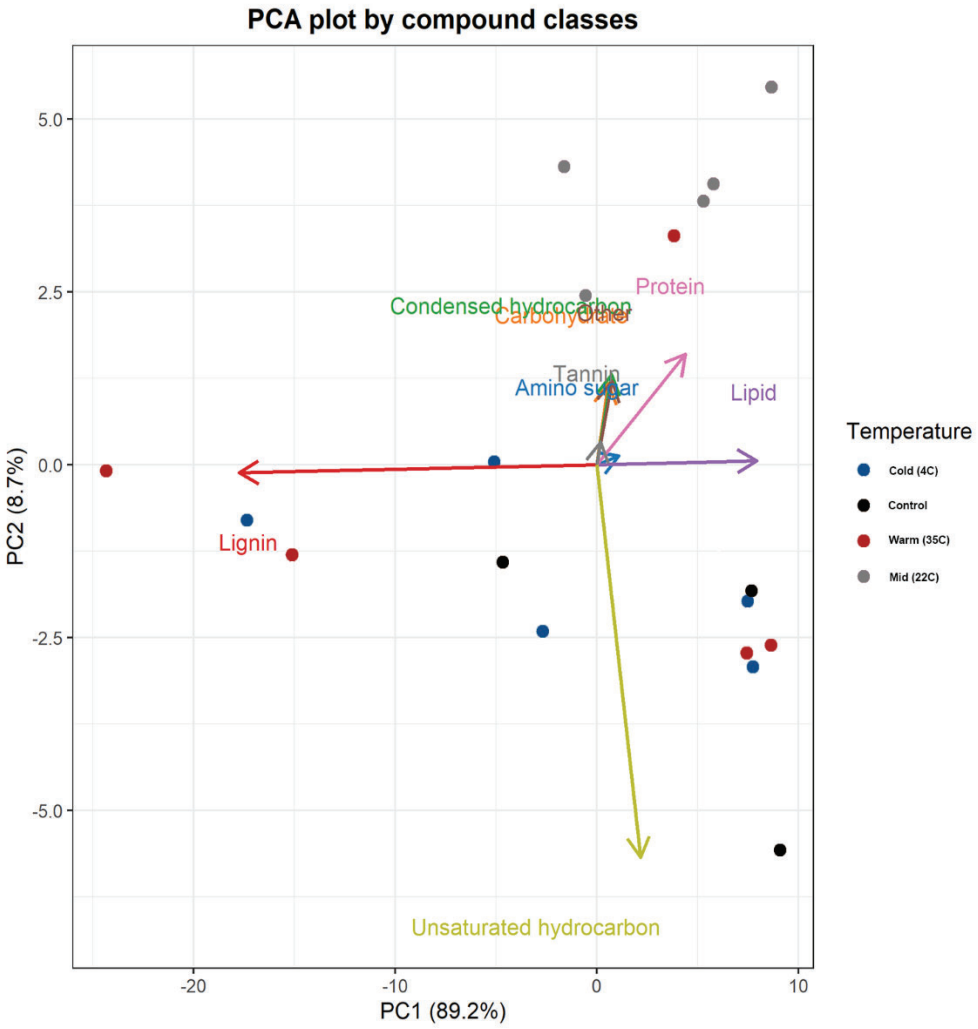

Figure 15: PCA plot showing differences in the compound classes present in each sample at different temperature treatments and which classes are responsible for the differences

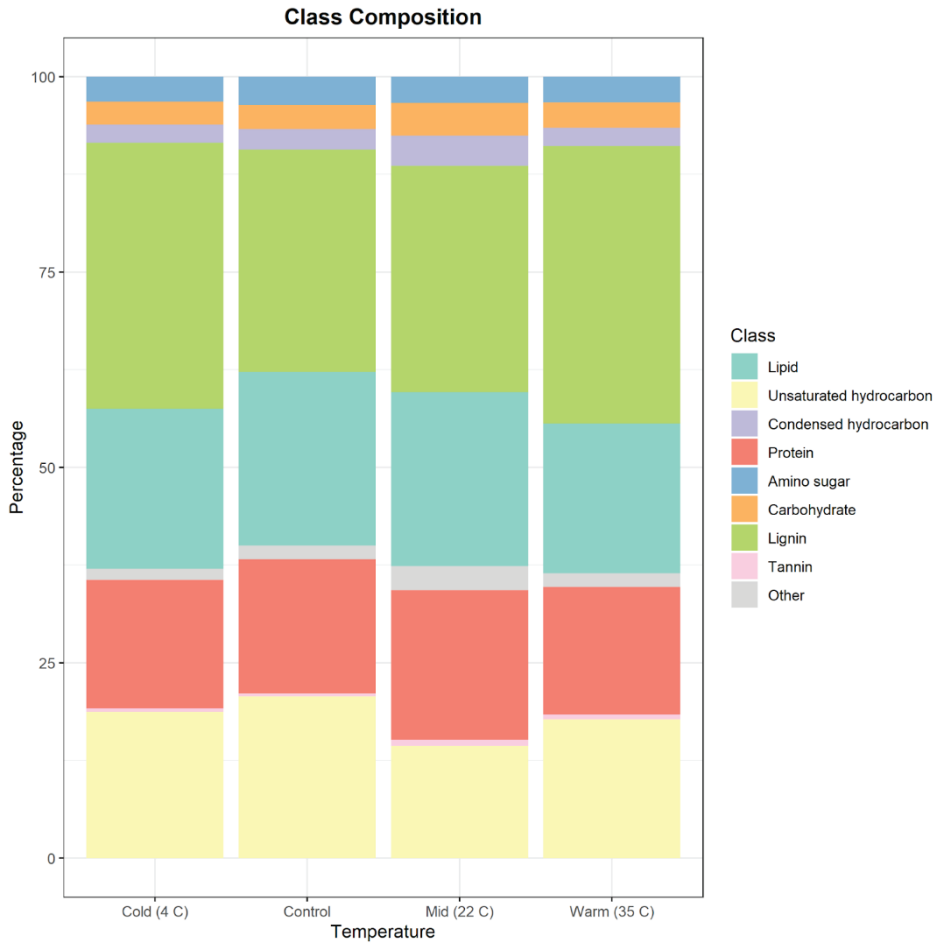

Figure 16: Differences in relative bulk metabolite class composition between the temperature treatments and controls

Figure 17 represents Gibbs free energy (GFE) violin plots comparing the GFE of the 22 ℃ samples relative to the other temperature treatments and the controls. In every comparison, the difference in GFE relative to 22 ℃ was statistically significant (PERMANOVA, $P < 0.05$).

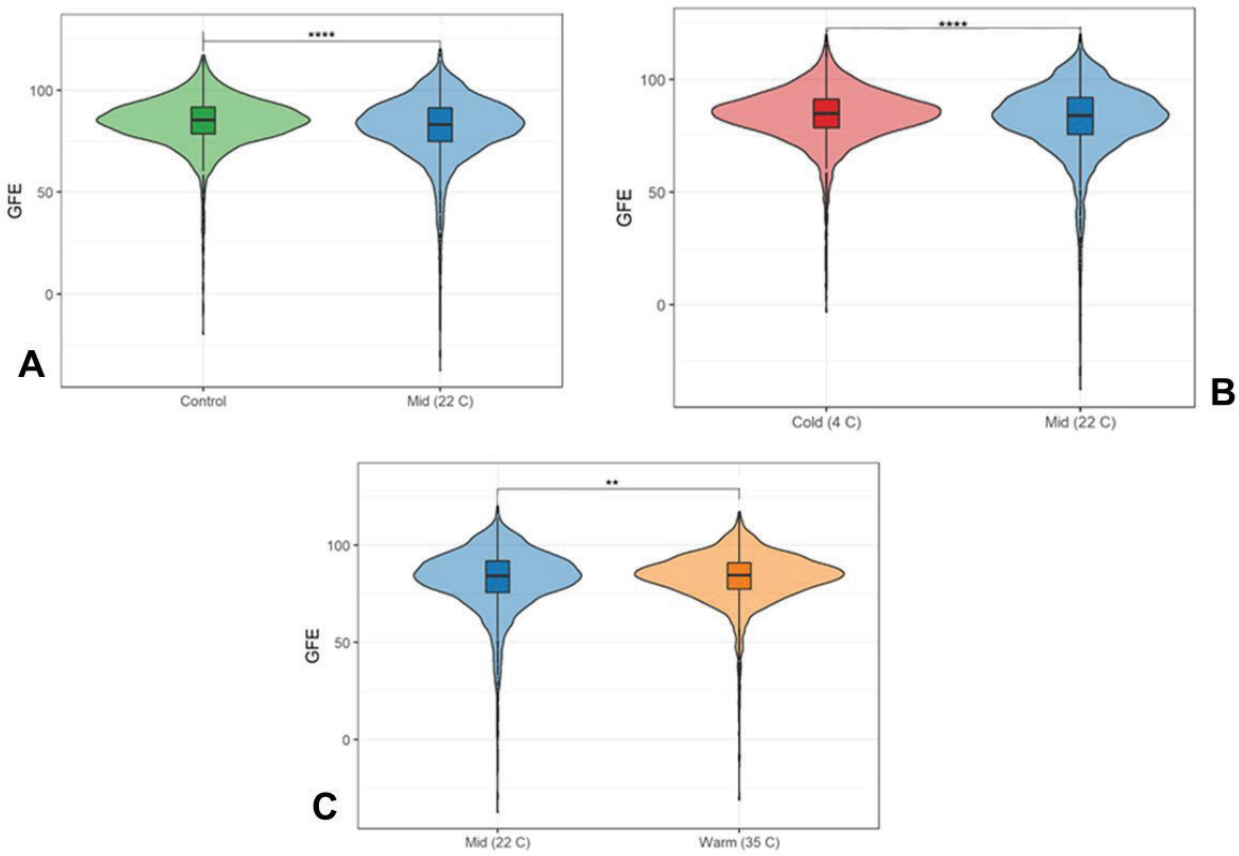

Figure 17. Violin plots showing the distribution of GFE at (A) controls vs 22 ℃, (B) 4 ℃ vs 22 ℃, and (C) 22 ℃ vs 35 ℃

With the exception of 4 °C versus 35 ℃, Figure 18A shows that the difference in aromaticity index between every pair is statistically significant ($p<0.05$). Both 4 °C and 35 ℃ samples showed an increase in aromaticity relative to the control. Conversely, 22 °C samples showed a decrease in aromaticity relative to the control.

Figure 18B shows that in pairwise comparisons between the different temperature treatments and the controls, all differences in DBE were statistically significant ($p<0.05$). Samples incubated at 4 ℃ and 35 ℃ show increased DBE relative to the control. 22 ℃ samples show decreased DBE relative to the control.

Along with describing information about the physical properties of the compounds in the samples, FTICR-MS data was used to determine the functional and abundance-based diversity of metabolites present at each temperature. Figure 18C shows functional diversity based on metabolite reactivity. Figure 18C shows that the functional reactivity was greater at 22 °C than at 4 ℃, 35 ℃, and the control. The 4 °C and 35 ℃ samples had similar means to each other and decreased reactivity relative to the control. However, there is much greater variation in functional reactivity at 35 °C. This variance can be understood when looking at the plates in Figure 13, which show the variation in bacterial growth on plates incubated at 35 ℃.

Abundance based diversity of the metabolites in each sample is visualized in Figure 18D. 22 ℃ samples had the greatest metabolite diversity abundance, 35 ℃ samples had the second highest, and 4 ℃ samples had a mean metabolite abundance that was less than both temperature treatments and the control. The cause of the extremely positive interquartile range at 4 ℃ is unknown.

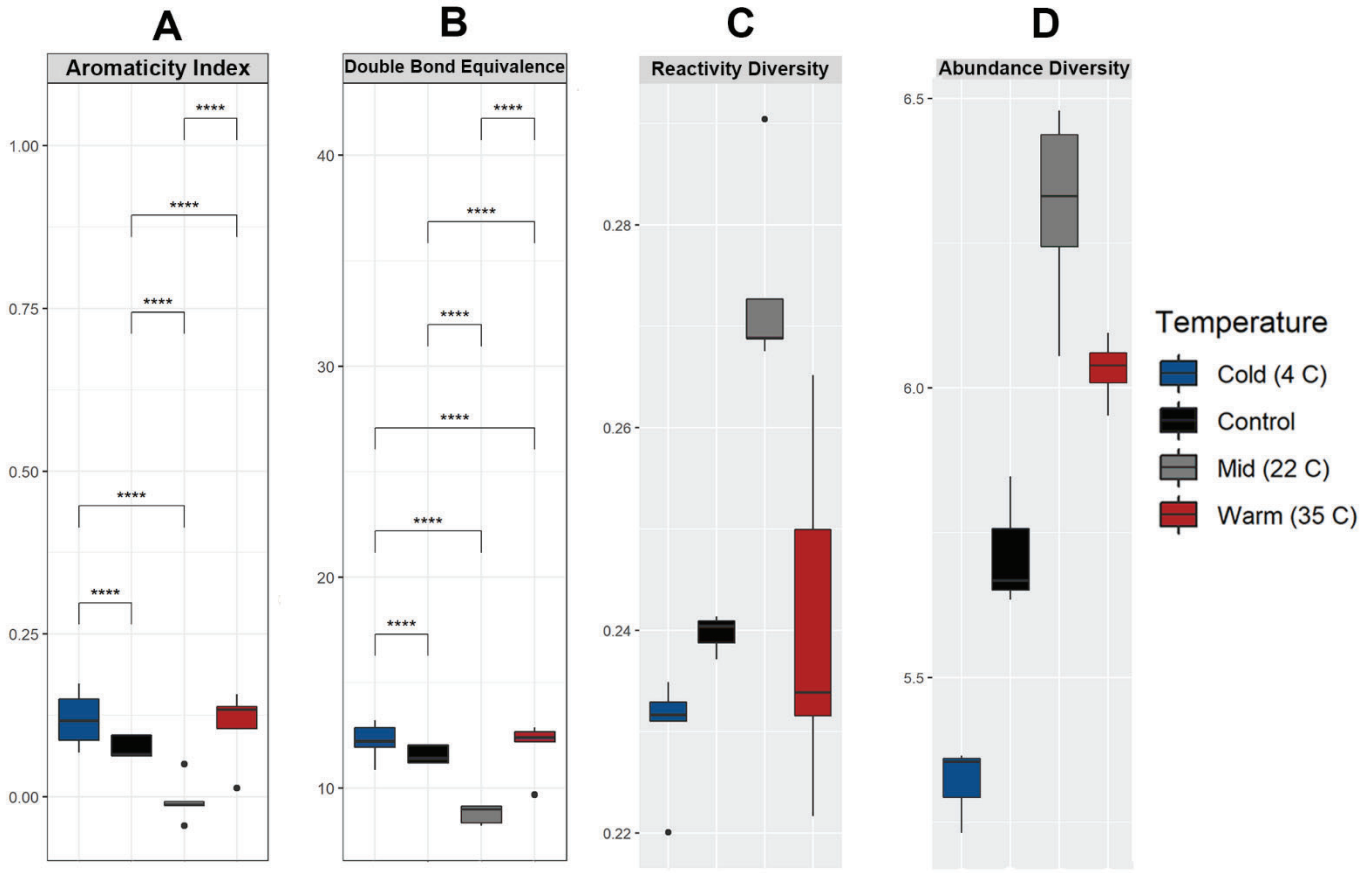

Figure 18. (A) Comparison of aromaticity index between each temperature treatment. (B) Comparison of double bond equivalence between each temperature treatment. (C) Comparison of diversity of reactivity of compounds present at each temperature treatment. (D) Comparison of abundance-based diversity of compounds present at each temperature treatment.

The abundance-based diversity data from Figure 18D was used in conjunction with the absorbance data from Figure 14 to generate Figure 19, which is a correlation plot relating cell density to metabolite diversity. The positive slope of the correlation line indicates that as bacterial abundance increased the metabolite diversity in the sample also increased. Figure 19 supports the hypothesis that bulk metabolite production is approximately proportional to bacterial growth.

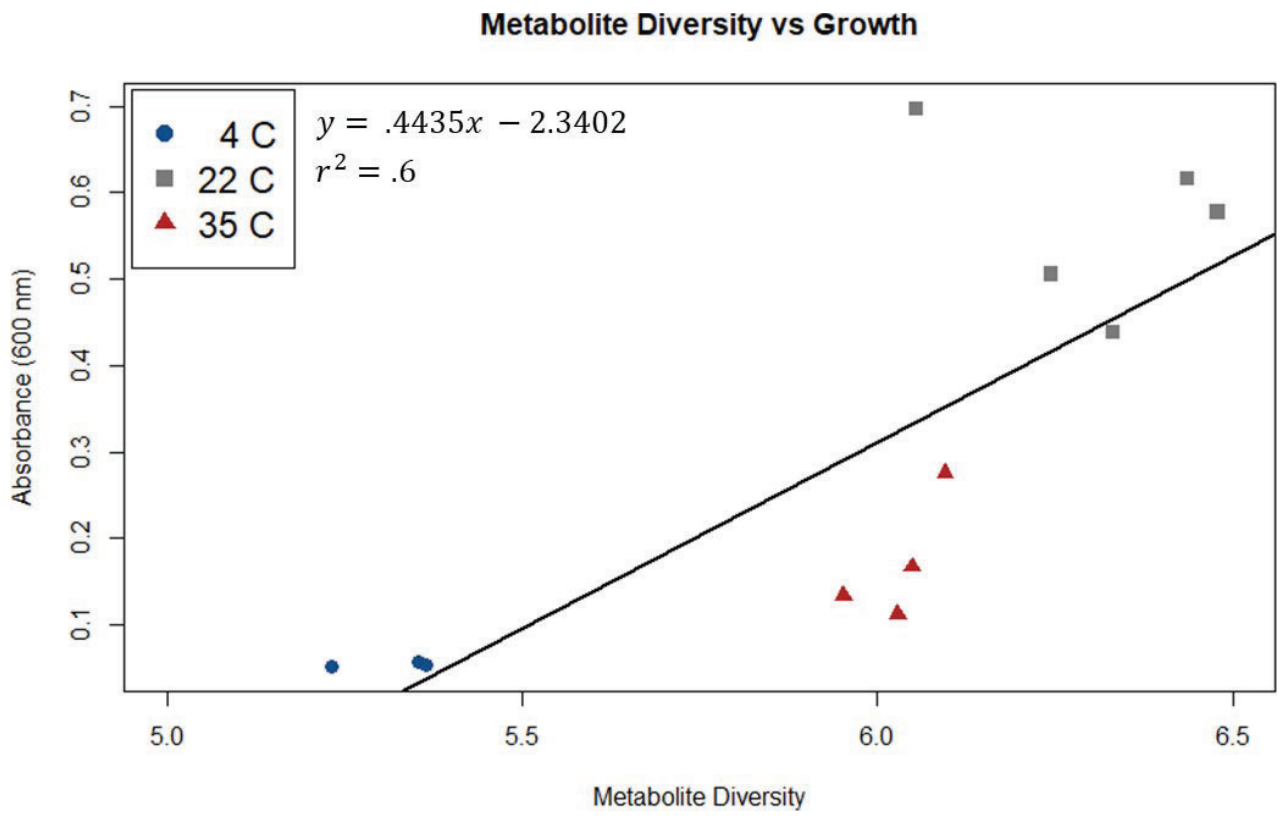

Figure 19. Scatter plot showing the positive correlation between bacterial abundance and metabolite diversity.

2.3.4 Metabolomics Data as Inferred from LC-MS/MS

Figure 20 is a dendrogram showing how similar each sample is to the others based on the metabolites present in each. A dendrogram was created for both RP and HILIC data, but they were identical so only one is shown. Figure 20 shows that all samples incubated at 22 ℃ and the two samples incubated at 35 ℃ that grew in biofilms were significantly different from the others. The 35 ℃ sample that grew two small colonies and one of the plates that grew in a sparse lawn were also different from the 4 ℃ samples and controls, but not significantly. One of the 35 ℃ plates that grew in a sparse lawn on the edge of the plate and all the 4 ℃ samples were most similar to the controls, showing there was not much bacterial activity, if any, in these samples.

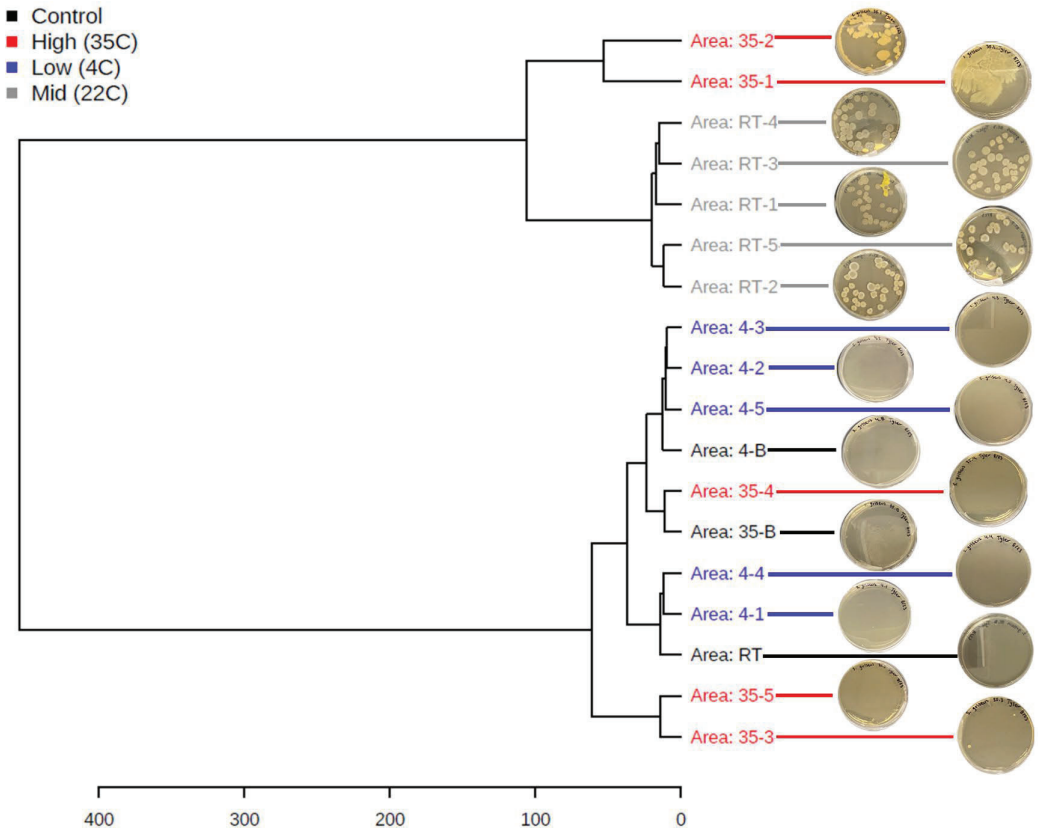

Figure 20. Scatter plot showing the positive correlation between bacterial abundance and metabolite diversity. Clustering result shown as a dendrogram with mapping to images of solid plates (distance measure using Euclidean and clustering algorithm using ward.D)

Heat maps were then used to identify broad patterns and compare similarities across the samples (Figure 21). All 22 ℃ samples and the biofilm forming 35 ℃ samples (in the right branch) were more similar to each other than to the other samples and controls. All of the 22 °C samples had nearly identical patterns relative to each other whereas there were some differences between the 22 ℃ samples and the two biofilm-forming 35 ℃ samples. Within the left-hand branch are the controls, 4 ℃ samples, and the three non-biofilm forming 35 ℃ samples. Two of the 35 °C samples in the left branch shared the majority of their patterns with the other samples in the left branch, but these two samples resemble the 22 ℃ samples in some places. With a few exceptions, the controls, 4 °C samples, and one of the 35 ℃ samples in the left branch all shared the same patterns.

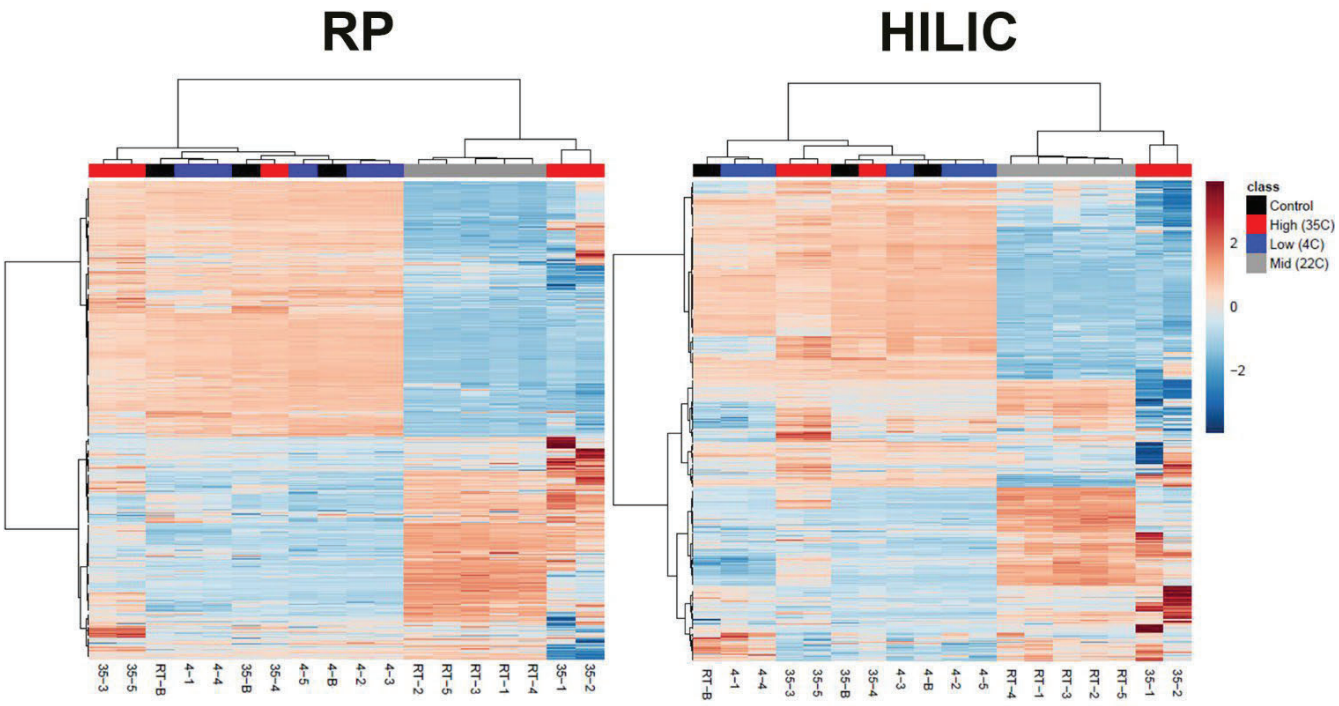

Figure 21. Clustering result shown as heatmap (distance measure using Euclidean, and clustering algorithm using ward.D). Labels on the x-axis relate to one inoculated plate. See Figure 20 for mapping to images of the plates.

Based on a t-test between 4 ℃ and the controls, there were no significant differences between compounds present at 4 ℃ and those present in the controls. Because there were no significant differences, investigations into upregulated compounds were only made between samples incubated at 22 ℃ and 35 ℃, both of which had features different from the media.

The volcano plots in Figure 22 show compounds that were up and downregulated at 35 ℃ relative to 22 ℃ (Log2fold change >1 and $p<0.05$). The top 50 features identified in each volcano plot were used to construct Table 2, which lists the name and function for the identified compound. Features that were not in any database or that have no known function were used to construct a Van Krevelen diagram (Figure 22C). The Van Krevelen diagram suggests that the upregulated unknown compounds were mostly phenol-, protein-, lipid-, and carbohydrate-like compounds.

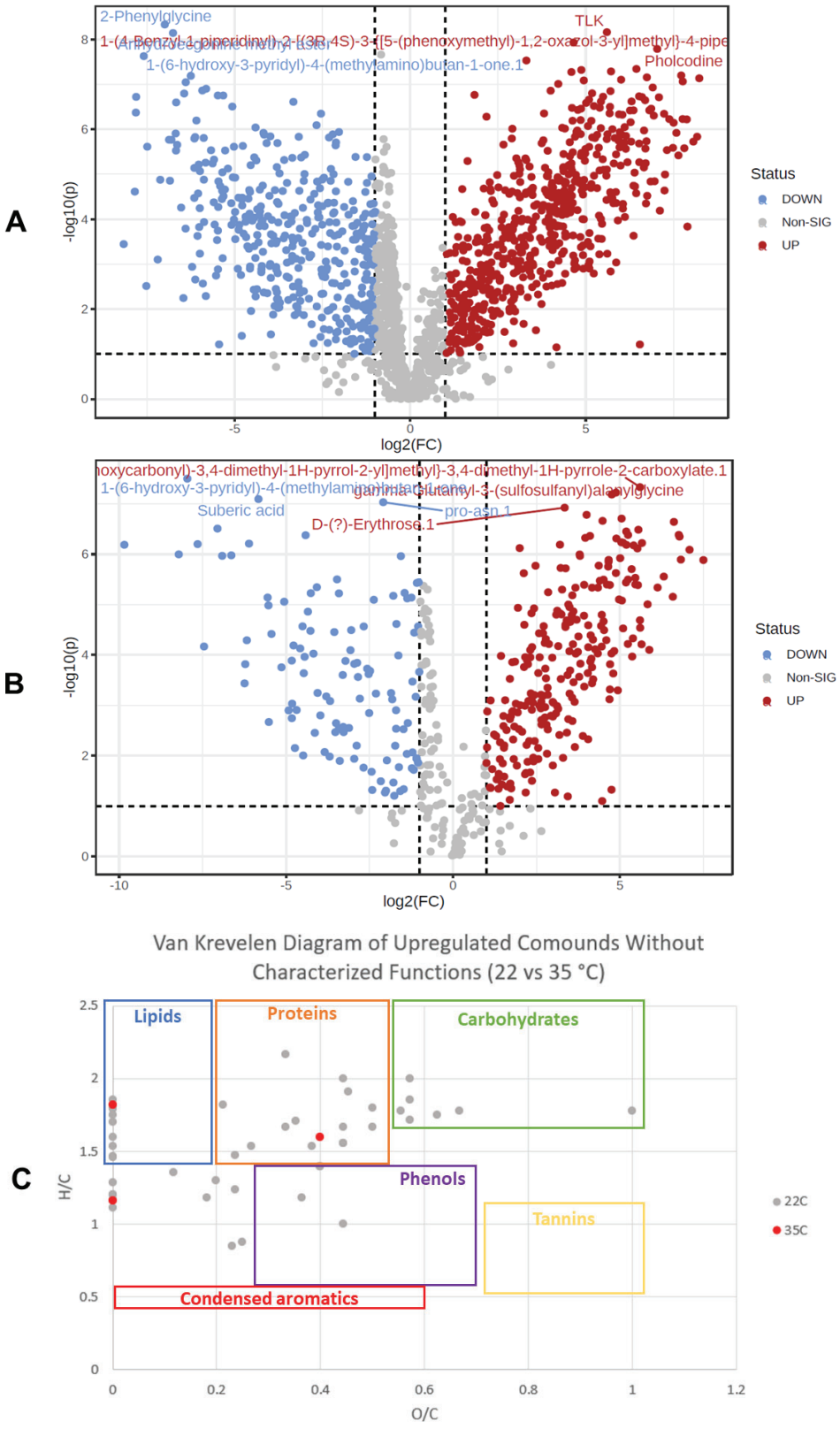

Figure 22. (A) RP volcano plot showing compounds upregulated at 35 °C (red), compounds upregulated at 22 °C (blue), and compounds that were insignificantly different between the two (gray). (B) Volcano plot made using HILIC data. (C) Van Krevelen diagram of compounds from the top 50 features in each volcano plot with no known function.

Table 2: Summary of compounds that were significantly upregulated at 35 ℃ vs 22 ℃ as inferred from the volcano plots in Figure 22 (gray highlight = upregulated at 22 ℃, red highlight = upregulated at 35 ℃)

Compound Name	Function	p-value	Separation	References
Cycloheximide	Antibiotic. Inhibits protein synthesis, a neuroprotective agent, an anticoronaviral agent, and a ferroptosis inhibitor	6.0×10^{-8}	HILIC	PubChem, 2022g
L-Ergothioneine	Antioxidant, helps in times of stress	6.7×10^{-7}	RP	Cumming et al., 2018
Streptidine	Functional parent of streptomycin	6.2×10^{-7}	RP	ChEBI, 2018e
2,3,4,5-tetrahydrodipicolinic acid	Involved in monobactam synthesis. Monobactams are antibiotics against gram negative bacteria	4.9×10^{-7}	RP	PubChem, 2022b
N-Acetyl-4-aminosalicylic acid	derived from salicylic acid, which is an antifungal agent and plant hormone	2.2×10^{-7}	HILIC	PubChem, 2022c
Hercynine	Involved in L-Ergothioneine biosynthesis pathway	6.6×10^{-6}	RP	PubChem, 2022m
Lycopsamine	Same as acetyllycopsamine	5.4×10^{-6}	HILIC	PubChem, 2022o
Cytidine 5'-monophosphate (hydrate)	Bacterial metabolite involved in RNA and DNA synthesis	5.1×10^{-6}	HILIC	ChEBI, 2018b
Acetyllycopsamine	Type of pyrrolizidine alkaloid, which are a class of compounds that are feeding deterrents and toxic compounds to generalist herbivores, including pests	4.3×10^{-6}	HILIC	PubChem, 2022d Nuringtyas et al., 2014

1D-3-amino-1-guanidino-1,3-dideoxy-scyllo-inositol	Involved in streptomycin production	2.4×10^{-6}	RP	PubChem, 2022a
DL-glutamine	Involved in peptidoglycan synthesis and recycling	1.9×10^{-6}	HILIC	PubChem, 2022k
D-raffinose	Trisaccharide, energy storage	1.6×10^{-6}	HILIC	PubChem, 2022r
Threonine	Amino acid	7.4×10^{-5}	HILIC	PubChem, 2022s
3-Ureidopropionic acid	Intermediate in uracil metabolism	6.8×10^{-5}	HILIC	ChEBI, 2018d
D-Alanyl-D-alanine	Component in peptidoglycan	4.3×10^{-5}	HILIC	PubChem, 2022i
Pro-tyr, glu-thr, gamma-glu-gln	Dipeptides	2.2×10^{-5} $- 1.7 \times 10^{-6}$	HILIC	PubChem, 2022q,l,j
Adefovir	Inhibits viral activity by inhibiting viral DNA pol, inhibiting viral penetration or uncoating, inhibiting viral protein synthesis, or blocking late stages of virus synthesis	1.85×10^{-5}	RP	PubChem, 2022e
DL-lactic acid	Evidence it aids plants growth	1.6×10^{-5}	HILIC	Böhme et al., 1998
DL-citrulline	Used in urea cycle and byproduct of nitric oxide production, nitric oxide helps plants respond to biotic/abiotic stress	7.8×10^{-4}	HILIC	ChEBI, 2018c Simontacchi et al., 2015

Cytidine	Used in RNA synthesis	7.4×10^{-4}	HILIC	PubChem, 2022h
Ornithine	Component of urea cycle, excess nitrogen storage	4.9×10^{-4}	HILIC	PubChem, 2022n
Harmine	Involved in beta-carboline synthesis, which is a class of chemicals with antiparisitic, antiviral, and antitumoral properties	3.8×10^{-4}	RP	Kukula-Koch & Widelski, 2017
Uridine monophosphate (UMP)	Various metabolic roles, used as monomer in RNA	1.0×10^{-4}	HILIC	PubChem, 2022t ChEBI, 2018f
Bicine	"Good's buffer", may help stabilize soil pH	.001	HILIC	PubChem, 2022f
Pro-hyp	Dipeptide	.013	HILIC	PubChem, 2022p

Because of the morphological differences among the 35 °C plates, an additional comparison was made between the 35 °C plates without biofilms and the 22 °C plates. Lactic acid was not upregulated at 35 °C without the presence of biofilms, suggesting it came solely from the biofilms. Additionally, indole-3-acetic acid (auxin) and alanylclavam (antibiotic) were upregulated at 22 °C relative to 35 °C without the biofilms. This suggests that the biofilms produce these compounds in sufficient amounts to make up for the lack of production in the samples that did not form biofilms.

2.4 Discussion

Solid and liquid media inoculated with *Streptomyces griseus* were incubated at three different temperatures to test the effect of temperature on its growth and metabolism. Using a combination of 600 nm spectrophotometry, FTICR-MS, and LC-MS/MS we found that that 22 °C is the optimal temperature for *S. griseus* growth. Bacteria incubated at 35 °C grew inconsistently and at a lower rate than those at 22 °C, in addition to producing fewer beneficial secondary metabolites. Incubation at 4 °C was suboptimal for *S. griseus* and slowed the activity of the bacteria significantly.

2.4.1 Solid and Liquid Culture Growth

Quantitative evidence from the growth curve confirmed the visual evidence from the solid plates that *S. griseus* grows in the greatest total amount and at the greatest rate at 22 ℃, then 35 ℃, and then 4 ℃, where there was no evidence of growth. The bacteria that grew in an abundant lawn morphology resembled a biofilm, so it is possible that some of the bacteria were able to initiate a biofilm formation pathway in an attempt to increase resilience to the heat stress (Lopez et al., 2010; Winn et al., 2014; Vinogradova et al., 2015). Winn et al. (2014) describes biofilm formation in *S. griseus* as "hyphae interlocking to create a thick mesh of cells". It is unclear why only two of the five inoculated plates would grow in a biofilm, but the lawn morphology became evident after only two days, suggesting that the genes required for biofilm formation were expressed early on. The 35 ℃ plates that did not grow in a biofilm may have failed to initiate this pathway early on and were unable to later because of the intense heat stress. The 35 ℃ plates that did not grow in a biofilm morphology did not grow in abundance, suggesting that biofilms are important for *S. griseus* growth and survival at high temperatures. However, the inconsistency of the lawn morphology shows that it is not a guaranteed trait at high temperatures, and in most cases *S. griseus* struggles to grow at elevated temperatures. Given the relatively small number of samples in this study, a future study investigating *S. griseus* biofilm formation at elevated temperatures could utilize more replicates to get a better understanding of biofilm formation frequency.

Another possibility is that the biofilms that formed at 35 ℃ were the result of contamination, not differential gene expression. To guarantee the biofilms were formed by *S. griseus* and not contamination, the sample would need to be sequenced or run in a gel and then compared to a known, pure sample of *S. griseus*. However, *S. griseus* is capable of forming biofilms and compounds known to be produced by this species like indole-3-acetic acid and alanylclavam were found in abundance in the biofilm forming samples; therefore these biofilms were likely formed by *S. griseus* and not an outside agent (Zelyas et al., 2008; Vurukonda et al., 2018). Additionally, all control plates remained free of bacteria through the entirety of the incubation period, suggesting proper sterile technique was used during inoculation and the plates were adequately sealed to prevent contamination from the environment infiltrating the plates.

One of the colonies on a plate incubated at 22 ℃ became surrounded by a yellow pigment after three days. One possible explanation for this is that some contamination got onto the plate during inoculation and grew into visibility after a few days. Another possibility is that the pigment was excreted by the bacterial colony at the pigments center. Ohnishi et al., 2003, describes the production of a yellow pigment by *S. griseus* under conditions of phosphate depletion. The description of the pigment by Ohnishi et al. matches what was seen in this experiment, but this experiment utilized rich media that should not have become phosphate depleted after only three days of incubation.

2.4.2 Metabolomics Data as Inferred from FTICR-MS

FTICR-MS data characterizes bulk metabolite composition within the samples. Much of the FTICR-MS data reinforces the plating and growth curve results. The increases in the abundance of protein- and carbohydrate-like compounds at 22 ℃ were indicators that the bacteria were thriving. These molecules are indicative of growth because proteins have a wide range of metabolic uses and carbohydrates are used to store and supply energy to the cell (Lumen, n.d.; Revilla et al., n.d.). Proteins and carbohydrates are a part of primary metabolic pathways, so their upregulation is indicative of greater growth (Saltveit, 2018).

Relative to the 22 ℃ samples and the controls, samples incubated at 4 ℃ and 35 ℃ experienced increases in lignin-like or phenolic compounds. Phenolic compounds are often produced in response to biotic or abiotic stresses, as they can act as signals that induce internal defense mechanisms (Saltveit, 2018). Despite the lack of growth at 4 ℃, the increase in phenols at this temperature is likely due to bacterial activity very early on in the incubation period. The bacteria recognized the suboptimal temperature and started to produce phenols in response to the stress but were unable to adapt to the temperature and grow like the bacteria at 35 ℃.

Of the three temperature treatments, samples incubated at 22 ℃ had the most negative GFE, then 35 ℃, followed by the 4 ℃ samples, which had almost exclusively positive GFE. This means that more catabolic reactions are occurring at 22 ℃ than the other temperatures. Catabolic reactions are meant to

produce energy for building compounds like proteins, lipids, carbohydrates, and secondary metabolites. Samples incubated at 35 ℃ had a similar but more positive GFE pattern than 22 ℃ samples, again indicating growth, but at a reduced rate. Samples at 4 °C which showed no growth had almost no negative GFE, despite control samples having negative GFE values. This is likely explained by the increase in phenols at 4 °C, which would require energy to produce. Because the bacteria at 4 ℃ were not growing, they catabolized low NOSC compounds in the media to provide the energy to build phenols, but then did not grow enough to build carbohydrates and simple sugars that would result in negative GFE.

The increase in aromaticity index and DBE at 4 ℃ and 35 ℃ relative to the controls is likely due to the production of phenolic compounds, once again indicating that the bacteria were stressed at these temperatures. The decrease in these two metrics at 22 ℃ relative to the controls is likely due to the bacteria building peptides and sugars, which is indicative of microbial growth.

The functional based diversity displays the diversity in the reactivity of the metabolites in a sample. The elevated functional diversity observed at 22 ℃ is indicative of microbial activity because it shows that compounds are actively undergoing reactions and that a wide range of compounds are being produced that were not originally in the media. The decrease in functional diversity at 4 ℃ and 35 ℃ relative to the control is likely partially due to the bacteria investing in phenol production. This decrease is also indicative of stress. When bacteria are stressed, only primary metabolic pathways are active, limiting the functional diversity of the compounds produced. The large variation at 35 ℃ aligns with what was seen on the solid plates, where two of the plates had lots of growth, and therefore higher functional diversity, and the remaining plates had very minimal growth, and therefore lower functional diversity.

The abundance-based diversity is a measure of the diversity in the type of metabolite present in the sample. The increase in metabolite diversity at 22 ℃ indicates the bacteria are thriving because they are creating a wide range of metabolites by utilizing primary and secondary metabolic pathways. Samples incubated at 35 ℃ also have increased metabolite diversity relative to the control samples, indicating similar but reduced activity relative to at 22 ℃. This increase was likely carried by the two plates that formed biofilms. The decrease in metabolite diversity at 4 ℃ is likely because the bacteria increased phenol production and were stressed and only utilizing primary metabolic pathways.

2.4.3 Metabolomics Data as Inferred from LC-MS/MS

The heatmaps in Figure 21 show that even though the metabolic profiles of the 22 ℃ and 35 ℃ biofilm-forming samples were similar, there were discernible differences between them. This means that even though the bacteria that formed biofilms were able to grow abundantly like the bacteria incubated at 22 ℃, the heat stress did cause differences in metabolite production. The patterns present at 4 ℃ and 35 ℃ in non-biofilm-forming samples are very similar to the controls, showing that there was limited bacterial activity. There were some differences between two of the non-biofilms 35 ℃ samples, the 4 ℃ samples, and controls, showing that even though there was not much growth in these two 35 ℃ samples, there was enough activity to differentiate them. Overall, four of the five plates incubated at 35 ℃ showed some degree of difference relative to the controls and the 4 ℃ samples, indicating the bacteria were able to adapt to heat stress and grow, albeit inconsistently.

Table 2 shows compounds upregulated at 35 °C and 22 ℃ relative to each other. Relative to 35 ℃, bacteria at 22 ℃ upregulated the production of compounds used in growth and energy storage, antimicrobial compounds, antioxidants, and the plant growth hormone N-acetyl-4-aminosalicylic acid. Relative to at 22 ℃, bacteria incubated at 35 ℃ upregulated lactic acid production and components involved in RNA production. The upregulation of components used in growth is more evidence that the bacteria at 22 ℃ were growing better than at 35 ℃ and the upregulation of energy storage compounds shows the bacteria were not just growing but were thriving. The upregulation of components involved in RNA production is likely driven by the media. In a comparison between the 22 °C and 4 ℃ samples, cytidine was upregulated at 4 ℃. Because there were no significant differences between 4 ℃ samples and the media, upregulation at 4 ℃ relative to 22 ℃ suggests this compound is present in high amounts in the media. Additionally, in a comparison between 35 °C and 4 °C samples, none of the transcription components mentioned above were significantly upregulated at 35 ℃ compared to at 4 ℃. Because there was also limited overall activity at 35

°C, this suggests that the compounds related to RNA production came primarily from the media.

The upregulation of antimicrobial agents at 22 °C means more of these compounds were produced at 22 °C than at 35 °C, suggesting that *S. griseus* will become less effective at defending plants from pathogens as global temperatures rise. Similarly, the upregulation of N-acetyl-4-aminosalicylic acid at 22 °C suggests *S. griseus* could become less effective at promoting plant growth as global temperatures rise. However, this is less true in the case of biofilm forming *S. griseus*.

Lactic acid was likely upregulated at 35 °C because of the biofilms. Research has shown that biofilms can generate local hypoxia, which would stimulate the Cori Cycle to produce lactic acid (Fox et al., 2014; Wu et al., 2018). Research by Böhme et al., 1998, provides evidence that lactic acid has positive effects on plant growth. Additionally, the production of indole-3-acetic acid and alanylclavam in 35 °C biofilms suggests that if *S. griseus* is able to form a biofilm it can provide multiple benefits to plants. Despite the downregulation of some antimicrobial agents and plant growth hormone N-acetyl-4-aminosalicylic acid in 35 °C biofilms relative to 22 °C, as long *S. griseus* forms a biofilm, it can provide some benefits to plants as *S. griseus* at 22 °C, although fewer still.

2.5 Conclusions

In accordance with the hypothesis, this experiment revealed that among the temperatures that were tested, *Streptomyces griseus* grows the best and produces the most abundant and diverse set of metabolites at 22 °C. At 35 °C, *S. griseus* grew inconsistently and produced fewer compounds that are beneficial for plant growth and protection. In cultures that were able to form a biofilm at 35 °C, *S. griseus* grew more and produced more plant beneficial metabolites than *S. griseus* that did not form biofilms at 35 °C. However, biofilm forming *S. griseus* still produced fewer plant beneficial metabolites than at 22 °C. These results suggest that as global temperatures rise, *S. griseus* will become less effective at protecting plants from pathogens and promoting growth.

Chapter 3: Implications and Future Directions

To decrease, or at the very least maintain current crop losses to pathogens, it will be important to improve or develop new pest and pathogen control methods as the rhizosphere may become a less effective agent in pest and pathogen control in the future, particularly if other rhizobacteria experience similar effects, but this would need to be confirmed with additional experiments. One potential group of experiments would be to repeat the methods described in this paper for other important rhizobacteria or a mix of rhizobacteria. This would give us insight into whether it is just *S. griseus* that will become less effective with rising temperatures or if the rhizosphere as a whole would become less effective. Additional analyses to this experiment could include gas measurements of VOC changes with temperature and DNA sequencing to gain further information on *S. griseus* biofilm forming genes. Another potential experiment would be to incubate rhizobacteria present in soil with plants to determine if association with a plant significantly increases resilience to elevated temperatures and alters the metabolic profile of the bacteria. This would require additional work involving isolated bacterial cultures and isolated plants to determine where the metabolites came from.

This research project contributes to our understanding of how *Streptomyces griseus* and the rhizosphere will respond to rising global temperatures. Through this work and future research projects, we will gain a better understanding of how future crop losses to pests and pathogens may be affected, guiding us towards solutions that will ensure global food security.

References

Ardrey, R. E. (2003). Liquid Chromatography. In *Liquid chromatography - mass spectrometry: An introduction* (pp. 7–31). essay, John Wiley & Sons. Retrieved from https://onlinelibrary-wiley-com.ezproxy2.library.arizona.edu/doi/book/10.1002/0470867299.

Ayala, C. (2021). *Welcome to MetaboDirect's documentation!* MetaboDirect. Retrieved April 18, 2022, from https://metabodirect.readthedocs.io/en/latest/index.html#

Bahureksa, W., Tfaily, M. M., Boiteau, R. M., Young, R. B., Logan, M. N., McKenna, A. M., & Borch, T. (2021). Soil organic matter characterization by fourier transform ion cyclotron resonance mass spectrometry (FTICR MS): A critical review of sample preparation, analysis, and Data Interpretation. *Environmental Science and Technology*, *55*(14), 9637–9656. https://doi.org/10.1021/acs.est.1c01135

Bakker, P. A. H. M., Berendsen, R. L., Doornbos, R. F., Wintermans, P. C. A., & Pieterse, C. M. J. (2013, May 30). *The rhizosphere revisited: Root microbiomics*. Frontiers in Plant Science. Retrieved April 18, 2022, from https://www.frontiersin.org/articles/10.3389/fpls.2013.00165/full

Böhme, M., Ouahid, A., & Shaban, N. (1998). Reaction of some vegetable crops to treatments with lactate as BIOREGULATOR and fertilizer. *Acta Horticulturae*, (514), 33–40. https://doi.org/10.17660/actahortic.2000.514.3

Blattner, F. R., Plunkett, G., Bloch, C. A., Perna, N. T., Burland, V., Riley, M., Collado-Vides, J., Glasner, J. D., Rode, C. K., Mayhew, G. F., Gregor, J., Davis, N. W., Kirkpatrick, H. A., Goeden, M. A., Rose, D. J., Mau, B., & Shao, Y. (1997). The complete genome sequence of *escherichia coli* K-12. *Science*, *277*(5331), 1453–1462. https://doi.org/10.1126/science.277.5331.1453

Buszewski, B., & Noga, S. (2011). Hydrophilic interaction liquid chromatography (hilic)—a powerful separation technique. *Analytical and Bioanalytical Chemistry*, *402*(1), 231–247. https://doi.org/10.1007/s00216-011-5308-5

Chace, D., & Sparkman, D. (2005). What is Mass Spectrometry? American Society of Mass Spectrometry.

Chakraborty, S., Tiedemann, A. V., & Teng, P. S. (2000). Climate change: Potential impact on plant diseases. *Environmental Pollution*, *108*(3), 317–326. https://doi.org/10.1016/s0269-7491(99)00210-9

ChEBI. (2018a). *Creatine*. CHEBI:16919 - creatine. Retrieved April 18, 2022, from https://www.ebi.ac.uk/chebi/searchId.do?chebiId=CHEBI%3A16919

ChEBI. (2018b). *Cytidine 5'-monophosphate (hydrate)*. Cytidine 5'-monophosphate (hydrate) (CHEBI:27405). Retrieved April 18, 2022, from https://www.ebi.ac.uk/chebi/searchId.do?chebiId=CHEBI:17361

ChEBI. (2018c). *DL-citrulline*. DL-citrulline (CHEBI:27405). Retrieved April 18, 2022, from https://www.ebi.ac.uk/chebi/searchId.do?chebiId=CHEBI:18211

ChEBI (2018d). *N-carbamoyl-β-alanine*. N-carbamoyl-beta-alanine (CHEBI:18261). Retrieved April 18, 2022, from https://www.ebi.ac.uk/chebi/searchId.do?chebiId=CHEBI%3A18261

ChEBI. (2018e). *Streptidine*. streptidine (CHEBI:27405). Retrieved April 18, 2022, from https://www.ebi.ac.uk/chebi/searchId.do?chebiId=CHEBI%3A27405

ChEBI. (2018f). *Uridine monophosphate*. Uridine monophosphate (CHEBI:27405). Retrieved April 18, 2022, from https://www.ebi.ac.uk/chebi/searchId.do?chebiId=CHEBI:16695

Contrepois, K., Jiang, L., & Snyder, M. (2015). Optimized analytical procedures for the untargeted metabolomic profiling of human urine and plasma by combining hydrophilic interaction (HILIC) and reverse-phase liquid chromatography (rplc)–mass spectrometry*. *Molecular and Cellular Proteomics*, *14*(6), 1684–1695. https://doi.org/10.1074/mcp.m114.046508

Cumming, B. M., Chinta, K. C., Reddy, V. P., & Steyn, A. J. C. (2018). Role of ergothioneine in Microbial Physiology and pathogenesis. *Antioxidants and Redox Signaling*, *28*(6), 431–444. https://doi.org/10.1089/ars.2017.7300

Danaei, M., Baghizadeh, A., Pourseyedi, S., Amini, J., & Yaghoobi, M. M. (2014). Biological control of plant fungal diseases using volatile substances of Streptomyces griseus. *Pelagia Research Library*, *4*(1), 334–339.

Deeble, V. J., Lindley, H. K., Fazeli, M. R., Cove, J. H., & Baumberg, S. (1995). Depression of streptomycin production by Streptomyces griseus at elevated growth temperature: Studies using gene fusions. *Microbiology*, *141*(10), 2511–2518. https://doi.org/10.1099/13500872-141-10-2511

Dettmer, K., Aronov, P. A., & Hammock, B. D. (2006). Mass spectrometry-based metabolomics. *Mass Spectrometry Reviews*, *26*(1), 51–78. https://doi.org/10.1002/mas.20108

Dunn, W., & Ellis, D. (2005). Metabolomics: Current analytical platforms and methodologies. *TrAC Trends in Analytical Chemistry*, *24*(4), 285–294. https://doi.org/10.1016/j.trac.2004.11.021

El Rassi, Z. (2021). Reversed-phase and hydrophobic interaction chromatography of carbohydrates and glycoconjugates. *Carbohydrate Analysis by Modern Liquid Phase Separation Techniques*, 35–124. https://doi.org/10.1016/b978-0-12-821447-3.00017-2

FAO. (2019). TRANSFORMING THE WORLD THROUGH FOOD AND AGRICULTURE. Food and Agriculture Organization.

FAO. (2019, April 3). *New standards to curb the global spread of plant pests and diseases*. Food and Agriculture Organization of the United Nations. Retrieved April 18, 2022, from https://www.fao.org/news/story/en/item/1187738/icode/

FAO. (2020, May 7). *Land use in agriculture by the numbers*. Food and Agriculture Organization of the United Nations. Retrieved April 18, 2022, from https://www.fao.org/sustainability/news/detail/en/c/1274219/

Fox, E. P., Cowley, E. S., Nobile, C. J., Hartooni, N., Newman, D. K., & Johnson, A. D. (2014). Anaerobic bacteria grow within candida albicans biofilms and induce biofilm formation in suspension cultures. *Current Biology*, *24*(20), 2411–2416. https://doi.org/10.1016/j.cub.2014.08.057

Goedhart, J., & Luijsterburg, M. (20n.d.). VolcaNoseR is a web app for creating, exploring, labeling and sharing volcano plots. *Scientific Reports*.

Grubbs, K. J., Biedermann, P. H., Suen, G., Adams, S. M., Moeller, J. A., Klassen, J. L., Goodwin, L. A., Woyke, T., Munk, A. C., Bruce, D., Detter, C., Tapia, R., Han, C. S., & Currie, C. R. (2011). Genome sequence of Streptomyces griseus strain XYLEBKG-1, an ambrosia beetle-associated actinomycete. *Journal of Bacteriology*, *193*(11), 2890–2891. https://doi.org/10.1128/jb.00330-11

Guillarme, D., & Veuthey, J.-L. (2017, March 16). *Alternative strategies to reversed-phase liquid chromatography for the analysis of pharmaceutical compounds*. American Pharmaceutical Review. Retrieved April 18, 2022, from https://www.americanpharmaceuticalreview.com/Featured-Articles/335456-Alternative-Strategies-to-Reversed-Phase-Liquid-Chromatography-for-the-Analysis-of-Pharmaceutical-Compounds/

Guo, A. C., Jewison, T., Wilson, M., Liu, Y., Knox, C., Djoumbou, Y., Lo, P., Mandal, R., Krishnamurthy, R., & Wishart, D. (2012). ECMDB: The E. coli Metabolome Database. *Nucleic Acids Research*. https://doi.org/10.1093/nar/gks992

IPCC, 2021: Summary for Policymakers. In: Climate Change 2021: The Physical Science Basis. Contribution of Working Group I to the Sixth Assessment Report of the Intergovernmental Panel on Climate Change [MassonDelmotte, V., P. Zhai, A. Pirani, S.L. Connors, C. Péan, S. Berger, N. Caud, Y. Chen, L. Goldfarb, M.I. Gomis, M. Huang, K. Leitzell, E. Lonnoy, J.B.R. Matthews, T.K. Maycock, T. Waterfield, O. Yelekçi, R. Yu, and B. Zhou (eds.)]. Cambridge University Press. In Press.

Ismail, B., & Nielsen, S. S. (2010). Basic principles of chromatography. *Food Analysis*, 473–498. https://doi.org/10.1007/978-1-4419-1478-1_27

Jensen, P. H., Mysling, S., Højrup, P., & Jensen, O. N. (2012). Glycopeptide enrichment for MALDI-TOF mass spectrometry analysis by hydrophilic interaction liquid chromatography solid phase extraction (Hilic SPE). *Mass Spectrometry of Glycoproteins*, 131–144. https://doi.org/10.1007/978-1-62703-146-2_10

Kailasam, S. (2021, May 17). *LC-MS – what is LC-MS, LC-MS analysis and LC-MS/MS*. Analysis & Separations from Technology Networks. Retrieved April 18, 2022, from

https://www.technologynetworks.com/analysis/articles/lc-ms-what-is-lc-ms-lc-ms-analysis-and-lc-msms-348238

Khan Academy. (2021). *Principles of chromatography | stationary phase (article)*. Khan Academy. Retrieved April 18, 2022, from https://www.khanacademy.org/science/class-11-chemistry-india/xfbb6cb8fc2bd00c8:in-in-organic-chemistry-some-basic-principles-and-techniques/xfbb6cb8fc2bd00c8:in-in-methods-of-purification-of-organic-compounds/a/principles-of-chromatography

Klinge, S., Voigts-Hoffmann, F., Leibundgut, M., & Ban, N. (2012, March 19). *Atomic structures of the eukaryotic ribosome*. Trends in Biochemical Sciences. Retrieved April 18, 2022, from https://www.sciencedirect.com/science/article/pii/S0968000412000229

Koch, B. P., & Dittmar, T. (2006). From mass to structure: An aromaticity index for high-resolution mass data of natural organic matter. *Rapid Communications in Mass Spectrometry*, *20*(5), 926–932. https://doi.org/10.1002/rcm.2386

Kornder, J. D. (2002, May 25). *Streptomycin revisited: Molecular action in the microbial cell*. Medical Hypotheses. Retrieved April 18, 2022, from https://www.sciencedirect.com/science/article/pii/S0306987701914501

Krishna, V., & Qaim, M. (2008, June 1). *https://onlinelibrary.wiley.com/doi/full/10.1111/j.1467-9353.2008.00402.x#R40*. Wiley Online Library. Retrieved April 18, 2022, from https://onlinelibrary.wiley.com/doi/full/10.1111/j.1467-9353.2008.00402.x#R40

Kukula-Koch, W. A., & Widelski, J. (2017). Alkaloids. *Pharmacognosy*, 163–198. https://doi.org/10.1016/b978-0-12-802104-0.00009-3

Lang, J. M., Pérez-Quintero, A. L., Koebnik, R., DuCharme, E., Sarra, S., Doucoure, H., Keita, I., Ziegle, J., Jacobs, J. M., Oliva, R., Koita, O., Szurek, B., Verdier, V., & Leach, J. E. (2019). A pathovar of xanthomonas oryzae infecting wild grasses provides insight into the evolution of pathogenicity in Rice Agroecosystems. *Frontiers in Plant Science*, *10*. https://doi.org/10.3389/fpls.2019.00507

Laxman, R. S., & More, S. (2002). Reduction of hexavalent chromium by Streptomyces griseus. *Minerals Engineering*, *15*(11), 831–837. https://doi.org/10.1016/s0892-6875(02)00128-0

Lee, M. Y., Kim, H. Y., Lee, S., Kim, J.-G., Suh, J.-W., & Lee, C. H. (2015). Metabolomics-based chemotaxonomic classification of streptomyces spp. and its correlation with antibacterial activity. *Journal of Microbiology and Biotechnology*, *25*(8), 1265–1274. https://doi.org/10.4014/jmb.1503.03005

Lomba, A., Buchadas, A., Honrado, J. P., & Moreira, F. (2019). Are we missing the big picture? unlocking the social-ecological resilience of high nature value farmlands to future climate change. *Climate Change Management*, 53–72. https://doi.org/10.1007/978-3-319-75004-0_4

Lopez, D., Vlamakis, H., & Kolter, R. (2010). Biofilms. *Cold Spring Harbor Perspectives in Biology*, *2*(7). https://doi.org/10.1101/cshperspect.a000398

Lugtenberg, B., & Kamilova, F. (2009). *Plant-growth-promoting rhizobacteria*. Annual Reviews. Retrieved April 18, 2022, from https://www.annualreviews.org/doi/pdf/10.1146/annurev.micro.62.081307.162918

Lumen. (n.d.). *Functions of Proteins*. Biology for Majors I. Retrieved April 18, 2022, from https://courses.lumenlearning.com/wm-biology1/chapter/reading-function-of-proteins/#:~:text=Proteins%20are%20a%20class%20of,(monomers)%20are%20amino%20acids.

Mahmuti, M., West, J. S., Watts, J., Gladders, P., & Fitt, B. D. L. (2011). Controlling crop disease contributes to both food security and climate change mitigation. *International Journal of Agricultural Sustainability*, *7*(3), 189–202. https://doi.org/10.3763/ijas.2009.0476

Mendes, R., Garbeva, P., & Raaijmakers, J. M. (2013). The rhizosphere microbiome: Significance of plant beneficial, plant pathogenic, and human pathogenic microorganisms. *FEMS Microbiology Reviews*, *37*(5), 634–663. https://doi.org/10.1111/1574-6976.12028

National Center for Biotechnology Information (2022a). PubChem Compound Summary for CID 5459885, 1D-3-amino-1-guanidino-1,3-dideoxy-scyllo-inositol. Retrieved April 18, 2022 from https://pubchem.ncbi.nlm.nih.gov/compound/1D-3-amino-1-guanidino-1_3-dideoxy-scyllo-inositol.

National Center for Biotechnology Information (2022b). PubChem Compound Summary for CID 632, 2,3,4,5-Tetrahydropyridine-2,6-dicarboxylic acid. Retrieved April 18, 2022 from https://pubchem.ncbi.nlm.nih.gov/compound/2_3_4_5-Tetrahydropyridine-2_6-dicarboxylic-acid.

National Center for Biotechnology Information (2022c). PubChem Compound Summary for CID 65509, 4-Acetamidosalicylic acid. Retrieved April 18, 2022 from https://pubchem.ncbi.nlm.nih.gov/compound/4-Acetamidosalicylic-acid.

National Center for Biotechnology Information (2022d). PubChem Compound Summary for CID 156006, 7-Acetyllycopsamine. Retrieved April 18, 2022 from https://pubchem.ncbi.nlm.nih.gov/compound/7-Acetyllycopsamine.

National Center for Biotechnology Information (2022e). PubChem Compound Summary for CID 60172, Adefovir. Retrieved April 18, 2022 from https://pubchem.ncbi.nlm.nih.gov/compound/Adefovir.

National Center for Biotechnology Information (2022f). PubChem Compound Summary for CID 8761, Bicine. Retrieved April 18, 2022 from https://pubchem.ncbi.nlm.nih.gov/compound/Bicine.

National Center for Biotechnology Information (2022g). PubChem Compound Summary for CID 6197, Cycloheximide. Retrieved April 18, 2022 from https://pubchem.ncbi.nlm.nih.gov/compound/Cycloheximide.

National Center for Biotechnology Information (2022h). PubChem Compound Summary for CID 6175, Cytidine. Retrieved April 18, 2022 from https://pubchem.ncbi.nlm.nih.gov/compound/Cytidine.

National Center for Biotechnology Information (2022i). PubChem Compound Summary for CID 5460362, D-alanyl-D-alanine. Retrieved April 18, 2022 from https://pubchem.ncbi.nlm.nih.gov/compound/D-alanyl-D-alanine.

National Center for Biotechnology Information (2022j). PubChem Compound Summary for CID 150914, gamma-Glutamylglutamine. Retrieved April 18, 2022 from https://pubchem.ncbi.nlm.nih.gov/compound/gamma-Glutamylglutamine.

National Center for Biotechnology Information (2022k). PubChem Compound Summary for CID 738, DL-Glutamine. Retrieved April 18, 2022 from https://pubchem.ncbi.nlm.nih.gov/compound/DL-Glutamine.

National Center for Biotechnology Information (2022l). PubChem Compound Summary for CID 6998031, Glu-Thr. Retrieved April 18, 2022 from https://pubchem.ncbi.nlm.nih.gov/compound/Glu-Thr.

National Center for Biotechnology Information (2022m). PubChem Compound Summary for CID 5459798, Hercynine. Retrieved April 18, 2022 from https://pubchem.ncbi.nlm.nih.gov/compound/Hercynine.

National Center for Biotechnology Information (2022n). PubChem Compound Summary for CID 6262, L-ornithine. Retrieved April 18, 2022 from https://pubchem.ncbi.nlm.nih.gov/compound/L-ornithine.

National Center for Biotechnology Information (2022o). PubChem Compound Summary for CID 107938, Lycopsamine. Retrieved April 18, 2022 from https://pubchem.ncbi.nlm.nih.gov/compound/Lycopsamine.

National Center for Biotechnology Information (2022p). PubChem Compound Summary for CID 11902893, Prolylhydroxyproline. Retrieved April 18, 2022 from https://pubchem.ncbi.nlm.nih.gov/compound/Prolylhydroxyproline.

National Center for Biotechnology Information (2022q). PubChem Compound Summary for CID 152264, Prolyl-tyrosine. Retrieved April 18, 2022 from https://pubchem.ncbi.nlm.nih.gov/compound/Prolyl-tyrosine.

National Center for Biotechnology Information (2022r). PubChem Compound Summary for CID 439242, Raffinose. Retrieved April 18, 2022 from https://pubchem.ncbi.nlm.nih.gov/compound/Raffinose.

National Center for Biotechnology Information (2022s). PubChem Compound Summary for CID 6288, l-Threonine. Retrieved April 18, 2022 from https://pubchem.ncbi.nlm.nih.gov/compound/l-Threonine.

National Center for Biotechnology Information (2022t). PubChem Compound Summary for CID 6030, Uridine-5'-monophosphate. Retrieved April 18, 2022 from https://pubchem.ncbi.nlm.nih.gov/compound/Uridine-5_-monophosphate.

Newton, A. C., Johnson, S. N., & Gregory, P. J. (2011, January 30). *Implications of climate change for diseases, crop yields and food security - euphytica*. SpringerLink. Retrieved April 18, 2022, from https://link.springer.com/article/10.1007/s10681-011-0359-4

Nuringtyas, T. R., Verpoorte, R., Klinkhamer, P. G., van Oers, M. M., & Leiss, K. A. (2014). Toxicity of pyrrolizidine alkaloids to spodoptera exigua using insect cell lines and injection bioassays. *Journal of Chemical Ecology*, *40*(6), 609–616. https://doi.org/10.1007/s10886-014-0459-4

Ohnishi, Y., Furusho, Y., Higashi, T., Chun, H.-K., Horinouchi, S., Sakuda, S., & Furihata, K. (2003). Structures of Grixazone A and B, A-Factor-dependent Yellow Pigments Produced under Phosphate Depletion by Streptomyces griseus. *The Journal of Antibiotics*, *57*(3), 218–223. Retrieved from https://www.jstage.jst.go.jp/article/antibiotics1968/57/3/57_3_218/_pdf/-char/en.

Olanrewaju, O. S., & Babalola, O. O. (2018, December 29). *Streptomyces: Implications and interactions in plant growth promotion*. Applied microbiology and biotechnology. Retrieved April 18, 2022, from https://www.ncbi.nlm.nih.gov/pmc/articles/PMC6394478/

Peterson, B. L., & Cummings, B. S. (2005). A review of chromatographic methods for the assessment of phospholipids in biological samples. *Biomedical Chromatography*, *20*(3), 227–243. https://doi.org/10.1002/bmc.563

Poland, J., & Rutkoski, J. (2016). Advances and challenges in genomic selection for disease resistance. *Annual Review of Phytopathology*, *54*(1), 79–98. https://doi.org/10.1146/annurev-phyto-080615-100056

Rengel, Z. (2011). Soil Ph, Soil Health and Climate Change. *Soil Biology*, *29*, 69–85. https://doi.org/10.1007/978-3-642-20256-8_4

Revilla, M. K. F., Titchenal, A., Calabrese, A., Gibby, C., & Meinke, W. (2018). Carbohydrates. In *Human Nutrition* (pp. 141–168). essay, University of Hawai‘i at Mānoa. Retrieved from file:///C:/Users/trods/Downloads/Human-Nutrition-1531778509.pdf.

Saltveit, M. (2018). Synthesis and Metabolism of Phenolic Compounds. In E. Yahia (Ed.), *Fruit and Vegetable Phytochemicals: Chemistry and Human Health* (pp. 115–125). essay, Wiley Blackwell.

Shinkawa, H., Sugiyama, M., Hatada, Y., Ohuchi, T., Udagawa, M., & Nimi, O. (1994). SILENCE OF STREPTOMYCIN 6-PHOSPHOTRANSFERASE GENE DERIVED BY INCUBATION AT A HIGH TEMPERATURE IN STREPTOMYCES GRISEUS. *Biotechnology Letters*, *13*(8), 537–542. https://doi.org/10.1007/BF01033405

BioLibre (2021, January 3). Siderophores. https://bio.libretexts.org/@go/page/8840

Simontacchi, M., Galatro, A., Ramos-Artuso, F., & Santa-María, G. E. (2015). Plant survival in a changing environment: The role of nitric oxide in plant responses to abiotic stress. *Frontiers in Plant Science*, *6*. https://doi.org/10.3389/fpls.2015.00977

Sottorff, I., Wiese, J., Lipfert, M., Preußke, N., Sönnichsen, F. D., & Imhoff, J. F. (2019, June 6). *Different secondary metabolite profiles of phylogenetically almost identical streptomyces griseus strains originating from geographically remote locations*. Microorganisms. Retrieved April 18, 2022, from https://www.ncbi.nlm.nih.gov/pmc/articles/PMC6616549/

Suutari, M., & Laakso, S. (1992). Changes in fatty acid branching and unsaturation of Streptomyces griseus and brevibacterium fermentans as a response to growth temperature. *Applied and Environmental Microbiology*, *58*(7), 2338–2340. https://doi.org/10.1128/aem.58.7.2338-2340.1992

Tfaily, M. (2011). (dissertation). *Molecular characterization of dissolved organic matter in northern peatlands: Identifying the chemical signatures of climate change*. ProQuest. Retrieved from https://www.proquest.com/docview/993012654?fromopenview=true&pq-origsite=gscholar&parentSessionId=AawxJiueBCpUp%2BXEMJY%2Fcbf0FG7HT8Rbcs%2BpAnNe6hc%3D.

Tolić, N., Liu, Y., Liyu, A., Shen, Y., Tfaily, M. M., Kujawinski, E. B., Longnecker, K., Kuo, L.-J., Robinson, E. W., Paša-Tolić, L., & Hess, N. J. (2017). Formularity: Software for automated formula assignment of natural and other organic matter from ultrahigh-resolution mass spectra. *Analytical Chemistry*, *89*(23), 12659–12665. https://doi.org/10.1021/acs.analchem.7b03318

Trenberth, K. E. (2011). Changes in precipitation with climate change. *Climate Research*, *47*(1), 123–138. https://doi.org/10.3354/cr00953

Tubiello, F. N., Soussana, J.-F., & Howden, S. M. (2007). Crop and pasture response to climate change. *Proceedings of the National Academy of Sciences*, *104*(50), 19686–19690. https://doi.org/10.1073/pnas.0701728104

Tukey, H. B. (1966). Leaching of Metabolites from Above-Ground Plant Parts and Its Implications. *Torrey Botanical Society*, *93*(6), 385–401. Retrieved April 18, 2022, from https://www.jstor.org/stable/2483411?seq=1.

UCLA. (n.d.). *Double Bond Equivalent*. Illustrated glossary of organic chemistry. Retrieved April 18, 2022, from http://www.chem.ucla.edu/~harding/IGOC/D/double_bond_equivalent.html#:~:text=or%20Rings%5D'

United Nations. (2019, June 17). *Growing at a slower pace, world population is expected to reach 9.7 billion in 2050 and could peak at nearly 11 billion around 2100*. United Nations: Department of Economic and Social Affairs. Retrieved April 18, 2022, from https://www.un.org/development/desa/en/news/population/world-population-prospects-2019.html

United Nations. (2021). *Global Issues: Food*. United Nations. Retrieved April 18, 2022, from https://www.un.org/en/global-issues/food

Verpoorte, R., Choi, Y. H., Mustafa, N. R., & Kim, H. K. (2008). Metabolomics: Back to basics. *Phytochemistry Reviews*, *7*(3), 525–537. https://doi.org/10.1007/s11101-008-9091-7

Vurukonda, S. S. K. P., Giovanardi, D., & Stefani, E. (2018, March 22). *Plant growth promoting and biocontrol activity of Streptomyces spp. as endophytes*. International journal of molecular sciences. Retrieved April 18, 2022, from https://www.ncbi.nlm.nih.gov/pmc/articles/PMC5979581/

Waters, M., & Tadi, P. (2021, September 29). *Streptomycin - StatPearls - NCBI Bookshelf*. National Library of Medicine. Retrieved April 18, 2022, from https://www.ncbi.nlm.nih.gov/books/NB555886/

Wheeler, T., & von Braun, J. (2013). Climate change impacts on Global Food Security. *Science*, *341*(6145), 508–513. https://doi.org/10.1126/science.1239402

Winn, M., Casey, E., Habimana, O., & Murphy, C. D. (2014). Characteristics of streptomyces griseus biofilms in continuous flow tubular reactors. *FEMS Microbiology Letters*, *352*(2), 157–164. https://doi.org/10.1111/1574-6968.12378

Wu, Y., Klapper, I., & Stewart, P. S. (2018). Hypoxia arising from concerted oxygen consumption by neutrophils and microorganisms in biofilms. *Pathogens and Disease*, *76*(4). https://doi.org/10.1093/femspd/fty043

Wunderlich, S., & Gatto, K. A. (2015, November 10). *Consumer perception of genetically modified organisms and sources of information*. Oxford Academic. Retrieved April 18, 2022, from https://academic.oup.com/advances/article/6/6/842/4555145?login=true

Zelyas, N. J., Cai, H., Kwong, T., & Jensen, S. E. (2008). ALANYLCLAVAM biosynthetic genes are clustered together with one group of clavulanic acid biosynthetic genes in streptomyces clavuligerus. *Journal of Bacteriology*, *190*(24), 7957–7965. https://doi.org/10.1128/jb.00698-08